Digital Resonant Current Controllers for Voltage Source Converters

Author: Alejandro Gómez Yepes
Director: Jesús Doval Gandoy

Department of Electronics Technology, University of Vigo,

14 December 2011

Dissertation submitted for the degree of
Doctor of Philosophy at the University of Vigo

"Doctor Europeus" mention

Outline

Outline

Plant Model for Current-Controlled VSCs I

Model suitable for active filters, active rectifiers, adjustable speed drives (decoupled back EMF), etc.

$\boldsymbol{v_{\mathrm{ac}}}$: grid voltage, back EMF of electric machine, etc.

L filter

$$G_{\mathrm{L}}(s) = \frac{I(s)}{V_{\mathrm{C}}(s)} = \frac{1}{s\,L_{\mathrm{F}} + R_{\mathrm{F}}}$$

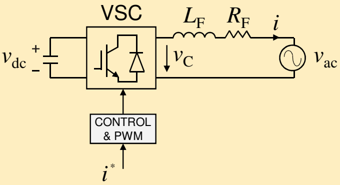

LCL filter

$$G_{\mathrm{LCL}}^{\mathrm{C}}(s) = \frac{I_{\mathrm{C}}(s)}{V_{\mathrm{C}}(s)};\; G_{\mathrm{LCL}}^{\mathrm{G}}(s) = \frac{I_{\mathrm{G}}(s)}{V_{\mathrm{C}}(s)}$$

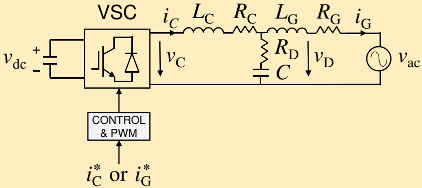

Pag. 3-7

Plant Model for Current-Controlled VSCs II

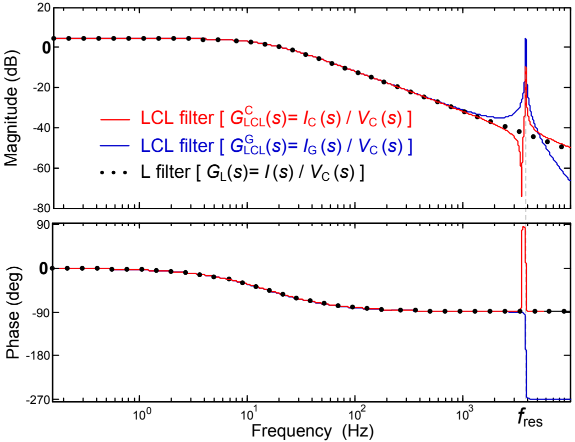

LCL filters behave as **L** at frequencies lower than approx. f_{res}:

$$G_{\text{LCL}}^{\text{C}}(s) \approx G_{\text{LCL}}^{\text{G}}(s) \approx$$

$$\approx \boldsymbol{G_{\text{L}}(s)} = \frac{1}{s\,L_{\text{F}} + R_{\text{F}}}$$

Pag. 3-7

Plant Model for Current-Controlled VSCs III

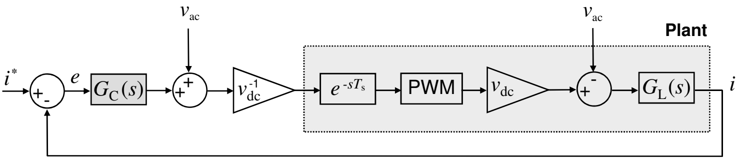

Complete block diagram

$\equiv$

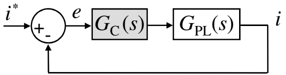

Simplified block diagram

- G_C: current controller
- G_L: L filter
- G_{PL}: plant model

$$G_{PL}(s) = \overbrace{e^{-sT_s}}^{\text{Comp. delay}} \overbrace{\frac{1-e^{-sT_s}}{s}}^{\text{ZOH (PWM)}} \overbrace{\frac{1}{s\,L_F + R_F}}^{G_L(s)}$$

$$G_{PL}(z) = \mathcal{Z}\left\{\mathcal{L}^{-1}\left[G_{PL}(s)\right]\right\} = \frac{z^{-2}}{R_F}\,\frac{1-\rho^{-1}}{1-z^{-1}\rho^{-1}} \quad \text{where} \quad \rho = e^{R_F T_s/L_F}$$

Plant Model for Current-Controlled VSCs III

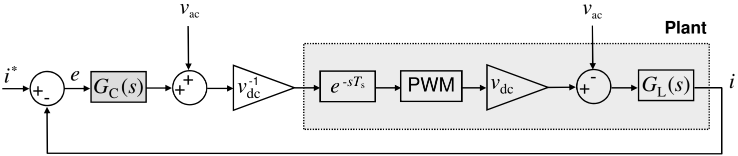

Complete block diagram

$\equiv$

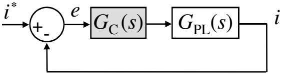

Simplified block diagram

- G_C: current controller
- G_L: L filter
- G_{PL}: plant model

$$G_{PL}(s) = \overbrace{e^{-sT_s}}^{\text{Comp. delay}} \overbrace{\frac{1-e^{-sT_s}}{s}}^{\text{ZOH (PWM)}} \overbrace{\frac{1}{s\,L_F + R_F}}^{G_L(s)}$$

$$G_{PL}(z) = \mathcal{Z}\left\{\mathcal{L}^{-1}\left[G_{PL}(s)\right]\right\} = \frac{z^{-2}}{R_F}\,\frac{1-\rho^{-1}}{1-z^{-1}\rho^{-1}} \quad \text{where} \quad \rho = e^{R_F T_s/L_F}$$

Hysteresis Control

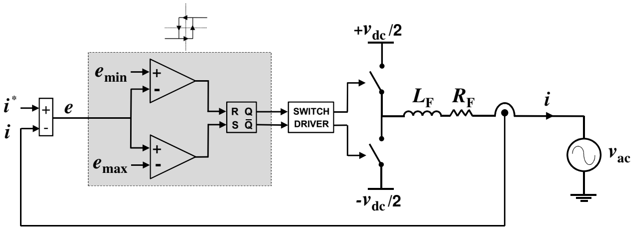

- **Simplicity**
- Unconditioned **stability**
- Very **fast** response
- Good **accuracy**

- **Variable switching frequency** (resonances, filters, power losses, ripple...)
- **Interference** among phases
- Inability to perform **selective** control
- Dependence on converter **topology**
- **Analog** comparators

Pag. 7-11

Hysteresis Control

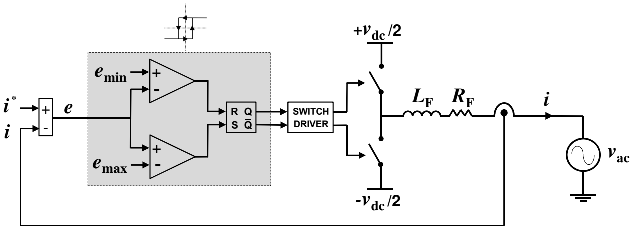

- **Simplicity**
- Unconditioned **stability**
- Very **fast** response
- Good **accuracy**

- **Variable switching frequency** (resonances, filters, power losses, ripple...)
- **Interference** among phases
- Inability to perform **selective** control
- Dependence on converter **topology**
- **Analog** comparators

Pag. 7-11

Deadbeat Control

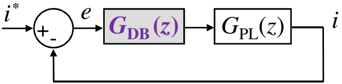

$$\frac{G_{\mathrm{DB}}(z)\, G_{\mathrm{PL}}(z)}{1 + G_{\mathrm{DB}}(z)\, G_{\mathrm{PL}}(z)} = z^{-2} \Rightarrow G_{\mathrm{DB}}(z) = \frac{R_{\mathrm{F}}}{1-\rho^{-1}} \, \frac{1 - z^{-1}\rho^{-1}}{1 - z^{-2}}$$

- **Simplicity**
- Theoretically, **fastest** transient among digital controllers

- Sensitiveness to deviations in **plant parameters**
- Need for v_{ac} **feedforward**
- Sensitiveness to measurement **noise**
- Need for **dead-times** compensation
- Closed-loop steady-state error

Pag.
11-12

PI Control in SRF

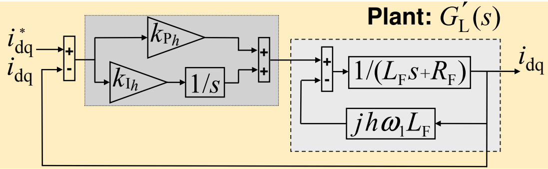

Conventional PI controller

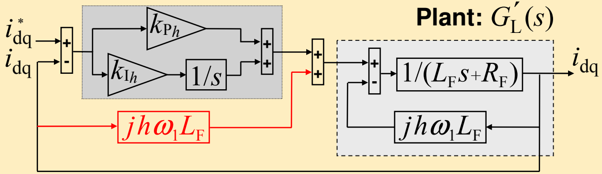

PI Controller with **cross-coupling decoupling** (PICCD)

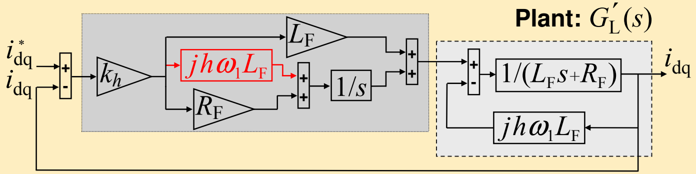

Complex-vector PI controller

Pag. 12-16

Repetitive Controllers

Common characteristics

- Tracking of **multiple** harmonics by a simple scheme
- Difficult **frequency adaptation**
- **Same parameters** for all peaks

Recursive form

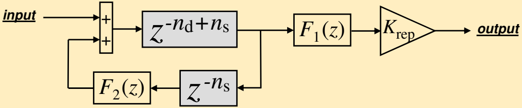

- No **selectiveness**
- Steady-state **error**
- Difficult **tuning**

DFT-based

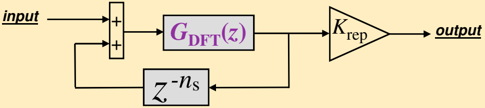

- **Selectiveness**
- No steady-state **error**

Pag. 17-23

Proportional+Resonant (PR) Controllers

Equivalent to a **conventional PI** in **positive-sequence SRF** + another one in **negative-sequence SRF**

Conventional **PI**:

$$\boldsymbol{G_{\mathrm{PI}_h}(s)} = k_{\mathrm{P}_h} + \frac{k_{\mathrm{I}_h}}{s}$$

Pos.seq. SRF: $\boldsymbol{G^{+}_{\mathrm{PI}_h}(s)} = G_{\mathrm{PI}_h}(s - jh\omega_1) = k_{\mathrm{P}_h} + \frac{k_{\mathrm{I}_h}}{s - jh\omega_1}$

Neg.seq. SRF: $\boldsymbol{G^{-}_{\mathrm{PI}_h}(s)} = G_{\mathrm{PI}_h}(s + jh\omega_1) = k_{\mathrm{P}_h} + \frac{k_{\mathrm{I}_h}}{s + jh\omega_1}$

$$\boldsymbol{G_{\mathrm{PR}_h}(s)} = G^{+}_{\mathrm{PI}_h}(s) + G^{-}_{\mathrm{PI}_h}(s) = \overbrace{2\,k_{\mathrm{P}_h}}^{K_{\mathrm{P}_h}} + \overbrace{2\,k_{\mathrm{I}_h}}^{K_{\mathrm{I}_h}} \frac{s}{s^2 + h^2\omega_1^2} = K_{\mathrm{P}_h} + K_{\mathrm{I}_h} \overbrace{\frac{s}{s^2 + h^2\omega_1^2}}^{R_{1_h}(s)}$$

Delay compensation: $\boldsymbol{G^{\mathrm{d}}_{\mathrm{PR}_h}(s)} = K_{\mathrm{P}_h} + K_{\mathrm{I}_h} \overbrace{\frac{s\,\cos(\phi'_h) - h\omega_1 \sin(\phi'_h)}{s^2 + h^2\omega_1^2}}^{R^{\mathrm{d}}_{1_h}(s)}$

Total controller: $\boldsymbol{G_{\mathrm{C}}(s)} = \sum_{h}^{n_h} G^{\mathrm{d}}_{\mathrm{PR}_h}(s) = \overbrace{\sum_{h}^{n_h} K_{\mathrm{P}_h}}^{K_{\mathrm{P_T}}} + \sum_{h}^{n_h} K_{\mathrm{I}_h}\, R^{\mathrm{d}}_{1_h}(s)$

Pag. 24-26

Proportional+Resonant (PR) Controllers

Equivalent to a **conventional PI** in **positive-sequence SRF** + another one in **negative-sequence SRF**

Conventional **PI**:

$$\boldsymbol{G}_{\mathbf{PI}_h}(\boldsymbol{s}) = k_{\mathrm{P}_h} + \frac{k_{\mathrm{I}_h}}{s}$$

$$\begin{cases} \text{Pos.seq. SRF} & \boldsymbol{G}^{+}_{\mathbf{PI}_h}(\boldsymbol{s}) = G_{\mathrm{PI}_h}(s - jh\omega_1) = k_{\mathrm{P}_h} + \frac{k_{\mathrm{I}_h}}{s - jh\omega_1} \\ \text{Neg.seq. SRF} & \boldsymbol{G}^{-}_{\mathbf{PI}_h}(\boldsymbol{s}) = G_{\mathrm{PI}_h}(s + jh\omega_1) = k_{\mathrm{P}_h} + \frac{k_{\mathrm{I}_h}}{s + jh\omega_1} \end{cases}$$

$$\boldsymbol{G}_{\mathbf{PR}_h}(\boldsymbol{s}) = G^{+}_{\mathrm{PI}_h}(s) + G^{-}_{\mathrm{PI}_h}(s) = \overbrace{2\,k_{\mathrm{P}_h}}^{K_{\mathrm{P}_h}} + \overbrace{2\,k_{\mathrm{I}_h}}^{K_{\mathrm{I}_h}} \frac{s}{s^2 + h^2\omega_1^2} = K_{\mathrm{P}_h} + K_{\mathrm{I}_h} \overbrace{\frac{s}{s^2 + h^2\omega_1^2}}^{R_{1_h}(s)}$$

Delay compensation:

$$\boldsymbol{G}^{\mathbf{d}}_{\mathbf{PR}_h}(\boldsymbol{s}) = K_{\mathrm{P}_h} + K_{\mathrm{I}_h} \frac{\overbrace{s\ \cos(\phi'_h) - h\omega_1 \sin(\phi'_h)}^{R^{\mathrm{d}}_{1_h}(s)}}{s^2 + h^2\omega_1^2}$$

Total controller:

$$\boldsymbol{G}_{\mathrm{C}}(\boldsymbol{s}) = \sum_{h}^{n_h} G^{\mathrm{d}}_{\mathrm{PR}_h}(s) = \overbrace{\sum_{h}^{n_h} K_{\mathrm{P}_h}}^{K_{\mathrm{P_T}}} + \sum_{h}^{n_h} K_{\mathrm{I}_h}\, R^{\mathrm{d}}_{1_h}(s)$$

Pag. 24-26

Proportional+Resonant (PR) Controllers

Equivalent to a **conventional PI** in **positive-sequence SRF** + another one in **negative-sequence SRF**

Conventional **PI**:

$$\boldsymbol{G_{\mathrm{PI}_h}(s)} = k_{\mathrm{P}_h} + \frac{k_{\mathrm{I}_h}}{s} \quad \begin{cases} \text{Pos.seq. SRF} & \boldsymbol{G^{+}_{\mathrm{PI}_h}(s)} = G_{\mathrm{PI}_h}(s - jh\omega_1) = k_{\mathrm{P}_h} + \frac{k_{\mathrm{I}_h}}{s - jh\omega_1} \\ \text{Neg.seq. SRF} & \boldsymbol{G^{-}_{\mathrm{PI}_h}(s)} = G_{\mathrm{PI}_h}(s + jh\omega_1) = k_{\mathrm{P}_h} + \frac{k_{\mathrm{I}_h}}{s + jh\omega_1} \end{cases}$$

$$\boldsymbol{G_{\mathrm{PR}_h}(s)} = G^{+}_{\mathrm{PI}_h}(s) + G^{-}_{\mathrm{PI}_h}(s) = \overbrace{2\,k_{\mathrm{P}_h}}^{K_{\mathrm{P}_h}} + \overbrace{2\,k_{\mathrm{I}_h}}^{K_{\mathrm{I}_h}} \frac{s}{s^2 + h^2\omega_1^2} = K_{\mathrm{P}_h} + K_{\mathrm{I}_h} \overbrace{\frac{s}{s^2 + h^2\omega_1^2}}^{R_{1_h}(s)}$$

Delay compensation: $$\boldsymbol{G^{\mathrm{d}}_{\mathrm{PR}_h}(s)} = K_{\mathrm{P}_h} + K_{\mathrm{I}_h} \overbrace{\frac{s\,\cos(\phi'_h) - h\omega_1 \sin(\phi'_h)}{s^2 + h^2\omega_1^2}}^{R^{\mathrm{d}}_{1_h}(s)}$$

Total controller: $$\boldsymbol{G_{\mathrm{C}}(s)} = \sum_{h}^{n_h} G^{\mathrm{d}}_{\mathrm{PR}_h}(s) = \overbrace{\sum_{h}^{n_h} K_{\mathrm{P}_h}}^{K_{\mathrm{P}_\mathrm{T}}} + \sum_{h}^{n_h} K_{\mathrm{I}_h}\, R^{\mathrm{d}}_{1_h}(s)$$

Pag. 24-26

Analysis and design of PR Controllers

Open-loop

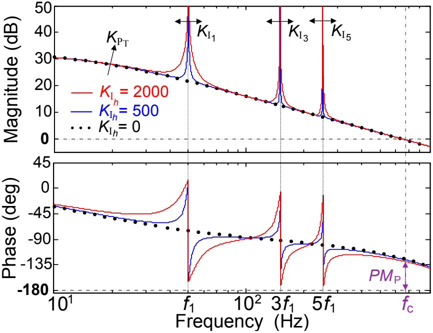

Closed-loop

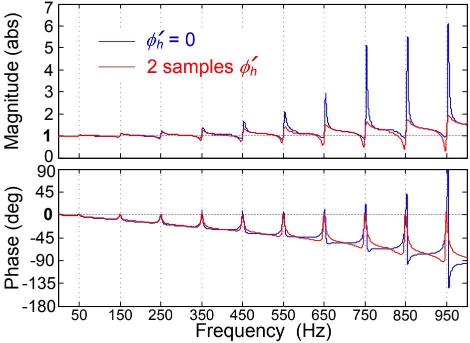

- $K_{P_T} \rightarrow f_c,\ PM_P$
- $K_{I_h} \rightarrow$ bandwidth around hf_1
- $hf_1 < f_c$ $\forall h$ such that $\phi_h' = 0$
- $\phi_h' \rightarrow$ anomalous peaks & stability

$$G_C(s) = K_{P_T} + \sum_{h}^{n_h} K_{I_h}\, R^{d}_{1_h}(s)$$

Pag.
32-36

Vector Proportional+Integral (VPI) Controllers

Equivalent to a **complex-vector PI** in **positive-sequence SRF** + another one in **negative-sequence SRF**

$$\boldsymbol{G_{\mathrm{VPI}_h}(s)} = \overbrace{G_{\mathrm{cPI}_h}(s - jh\omega_1)}^{G^{+}_{\mathrm{cPI}_h}} + \overbrace{G_{\mathrm{cPI}_h}(s + jh\omega_1)}^{G^{-}_{\mathrm{cPI}_h}} =$$

$$= K_{\mathrm{P}_h} \overbrace{\frac{s^2}{s^2 + h^2\omega_1^2}}^{R_{2_h}} + K_{\mathrm{I}_h} \overbrace{\frac{s}{s^2 + h^2\omega_1^2}}^{R_{1_h}} = K_h \frac{s\,(\overbrace{s\,L_{\mathrm{F}} + R_{\mathrm{F}}}^{\text{Plant cancellation}})}{s^2 + h^2\omega_1^2}$$

Delay compensation: $\boldsymbol{G^{\mathrm{d}}_{\mathrm{VPI}_h}(s)} = K_h \frac{(s\,L_{\mathrm{F}} + R_{\mathrm{F}})\left[s\,\cos(\phi'_h) - h\omega_1 \sin(\phi'_h)\right]}{s^2 + h^2\omega_1^2} =$

$$= K_{\mathrm{P}_h} \overbrace{\frac{s^2\cos(\phi'_h) - s\,h\omega_1\sin(\phi'_h)}{s^2 + h^2\omega_1^2}}^{R^{\mathrm{d}}_{2_h}(s)} + K_{\mathrm{I}_h} \overbrace{\frac{s\,\cos(\phi'_h) - h\omega_1\sin(\phi'_h)}{s^2 + h^2\omega_1^2}}^{R^{\mathrm{d}}_{1_h}(s)}$$

Pag. 26-27,53

Vector Proportional+Integral (VPI) Controllers

Equivalent to a **complex-vector PI** in **positive-sequence SRF** + another one in **negative-sequence SRF**

$$\boldsymbol{G_{\mathrm{VPI}_h}(s)} = \overbrace{G_{\mathrm{cPI}_h}(s - jh\omega_1)}^{G^{+}_{\mathrm{cPI}_h}} + \overbrace{G_{\mathrm{cPI}_h}(s + jh\omega_1)}^{G^{-}_{\mathrm{cPI}_h}} =$$

$$= K_{\mathrm{P}_h} \overbrace{\frac{s^2}{s^2 + h^2\omega_1^2}}^{R_{2_h}} + K_{\mathrm{I}_h} \overbrace{\frac{s}{s^2 + h^2\omega_1^2}}^{R_{1_h}} = K_h \frac{s\,(\overbrace{s\,L_{\mathrm{F}} + R_{\mathrm{F}}}^{\text{Plant cancellation}})}{s^2 + h^2\omega_1^2}$$

Delay compensation: $\boldsymbol{G^{\mathrm{d}}_{\mathrm{VPI}_h}(s)} = K_h \frac{(s\,L_{\mathrm{F}} + R_{\mathrm{F}})\left[s\,\cos(\phi'_h) - h\omega_1 \sin(\phi'_h)\right]}{s^2 + h^2\omega_1^2} =$

$$= K_{\mathrm{P}_h} \overbrace{\frac{s^2 \cos(\phi'_h) - s\,h\omega_1 \sin(\phi'_h)}{s^2 + h^2\omega_1^2}}^{R^{\mathrm{d}}_{2_h}(s)} + K_{\mathrm{I}_h} \overbrace{\frac{s\,\cos(\phi'_h) - h\omega_1 \sin(\phi'_h)}{s^2 + h^2\omega_1^2}}^{R^{\mathrm{d}}_{1_h}(s)}$$

Pag. 26-27,53

Analysis and design of VPI Controllers

Closed-loop

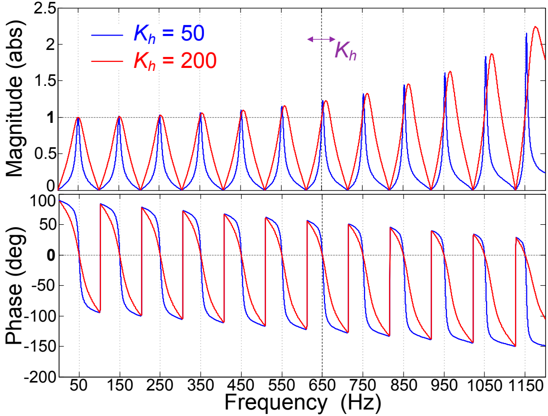

- $K_h \rightarrow$ **bandwidth** around hf_1
- $\phi'_h \rightarrow$ anomalous **peaks** & **stability** (only required at $\uparrow hf_1/f_s$)

Main Objectives of this PhD Thesis

- To provide an in-depth **study and comparison** of the effects of **discretization strategies**
- To develop **optimized discrete-time implementations** with a good tradeoff between
  - accuracy
  - resource-consumption & simplicity
- To propose an **analysis and design** methodology for resonant controllers by means of **Nyquist diagrams**, suitable for cases with more than one cross-over frequency.

Outline

Digital Implementations

1. Discretization of continuous **transfer function** (by Tustin, zero-pole matching, etc.)

2. Two discrete **integrators**
   - Direct int.: Forward Euler Feedback int.: Backward Euler **(f&b)**
   - Direct int.: Backward Euler Feedback int.: Backward Euler + z^{-1} **(b&b)**
   - Direct int.: Tustin Feedback int.: Tustin **(t&t)**

PR

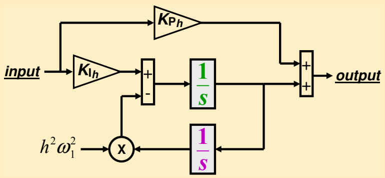

VPI

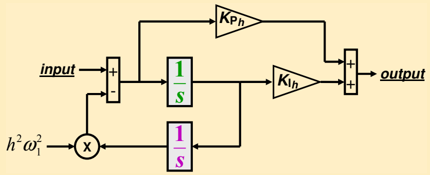

Pag. 43-45

Resonant Poles Displacement ($f_s = 10$ kHz)

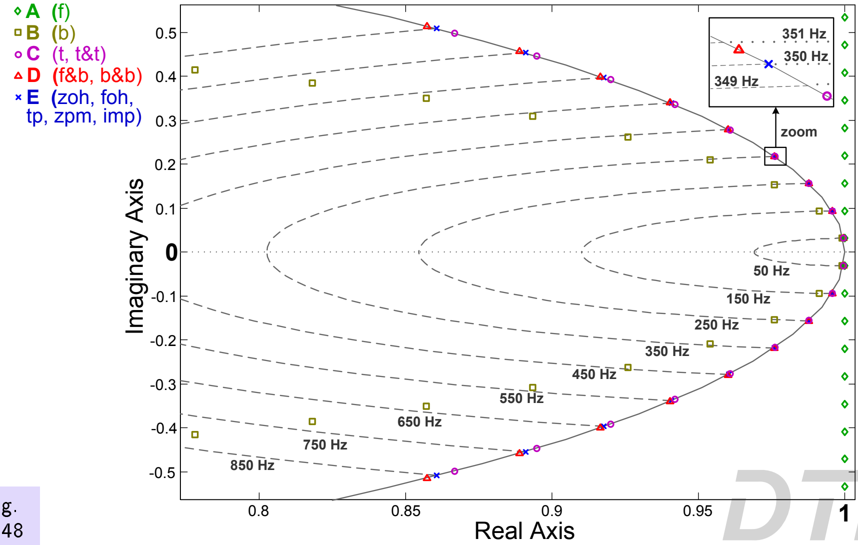

Pag.
45-48

Resonant Poles Displacement ($f_s = 10$ kHz)

- A (f)
- B (b)
- C (t, t&t)
- D (f&b, b&b)
- E (zoh, foh, tp, zpm, imp)

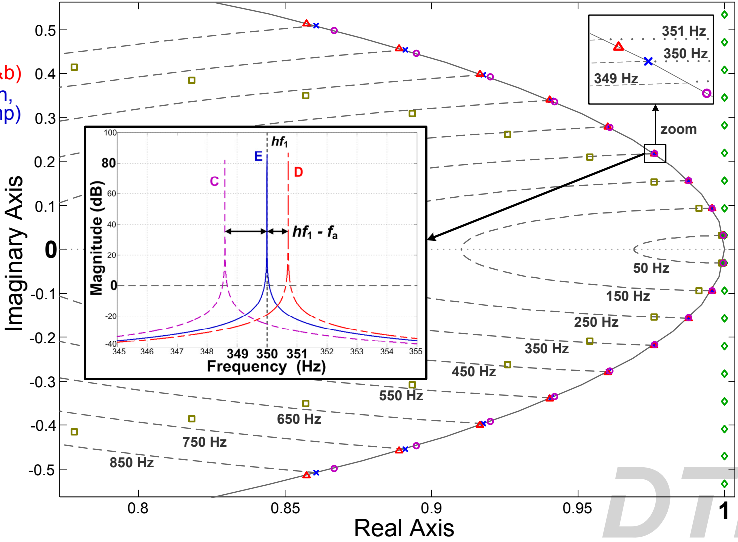

Pag. 45-48

Resonant Poles Displacement (variable f_s)

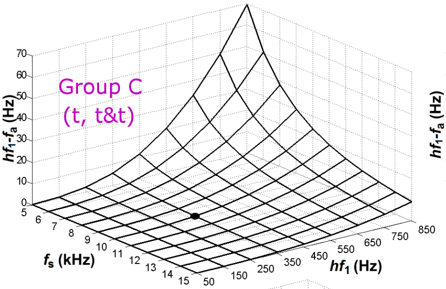

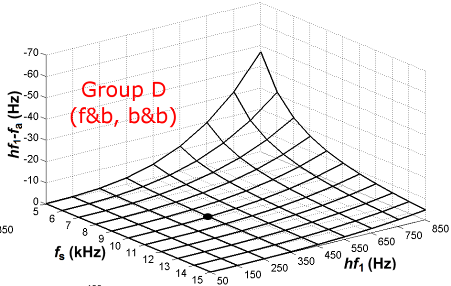

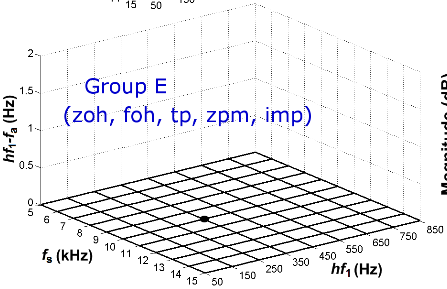

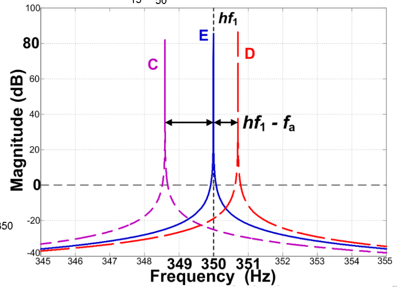

Pag.
45-48

Effects on Zeros of $R_{1_h}(s)$ (E methods)

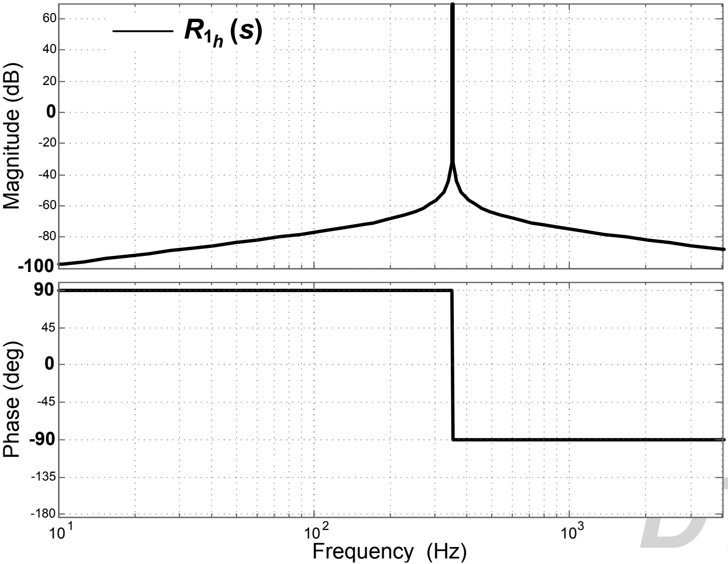

Pag. 48-50

Effects on Zeros of $R_{1_h}(s)$ (E methods)

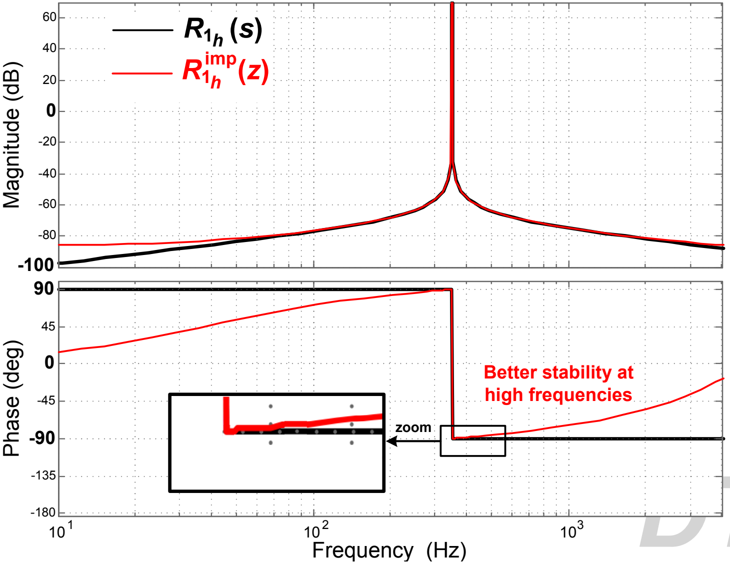

Pag. 48-50

Effects on Zeros of $R_{1_h}(s)$ (E methods)

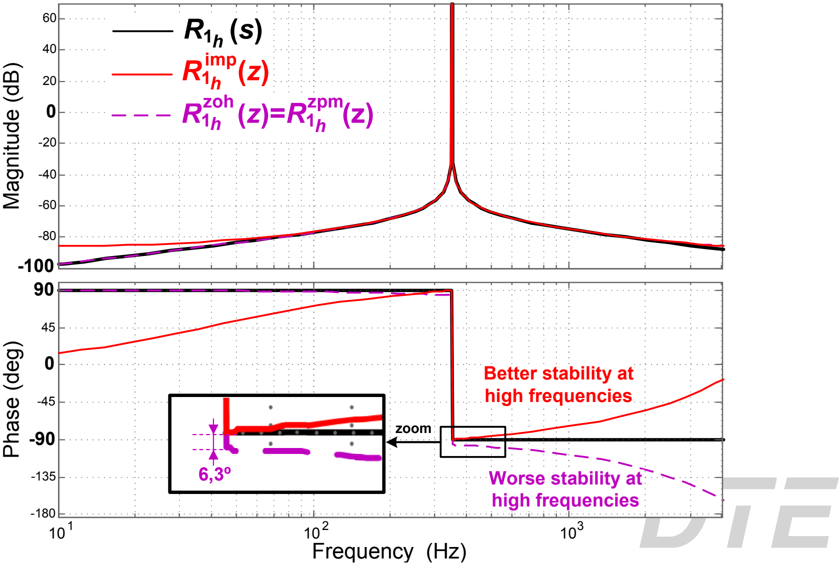

Pag. 48-50

Effects on Zeros of $R_{1_h}(s)$ (E methods)

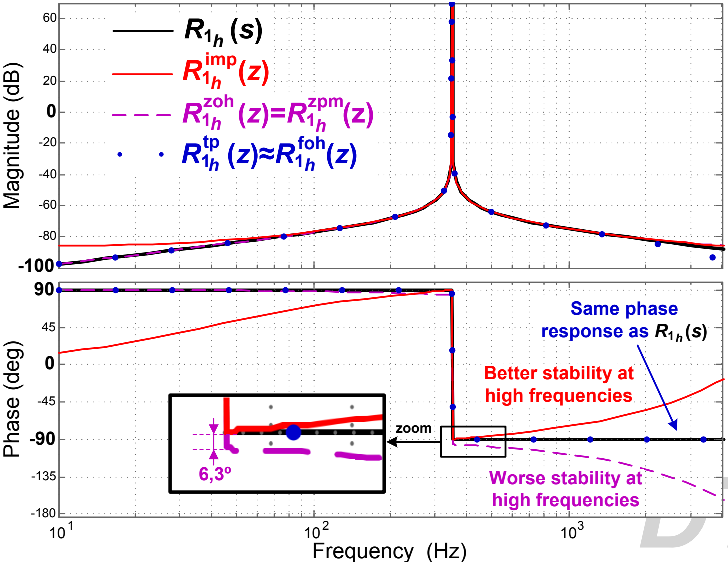

Pag. 48-50

Effects on Zeros of $R_{1_h}(s)$ (D methods)

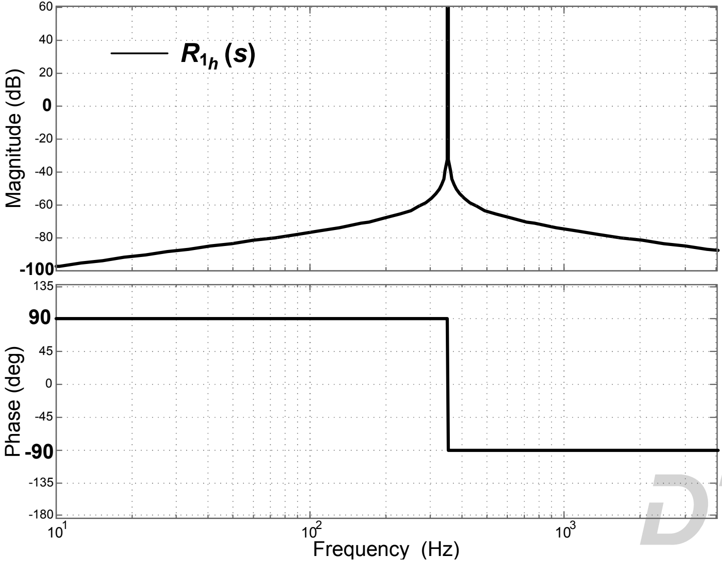

Pag. 50-51

Effects on Zeros of $R_{1_h}(s)$ (D methods)

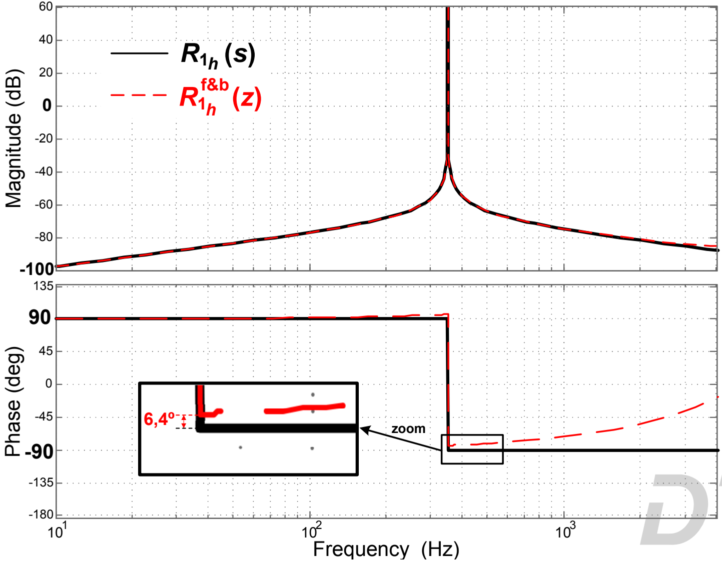

Pag. 50-51

Effects on Zeros of $R_{1_h}(s)$ (D methods)

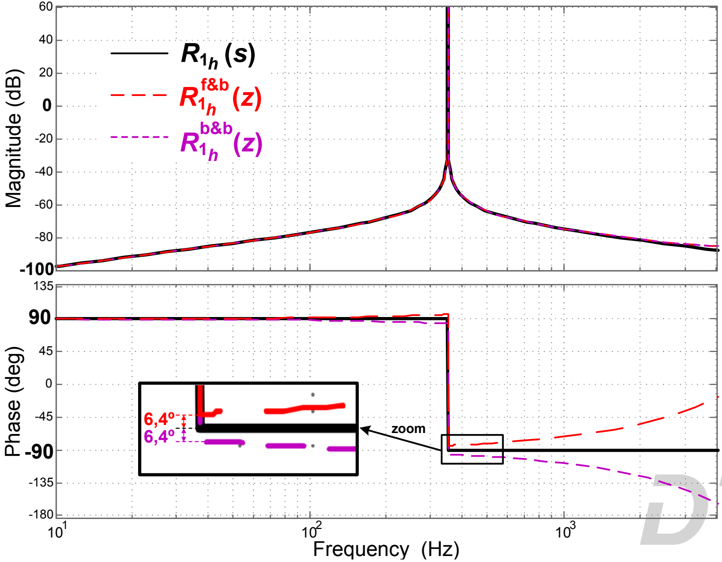

Pag. 50-51

Effects on Zeros of $R_{2_h}(s)$ (E methods)

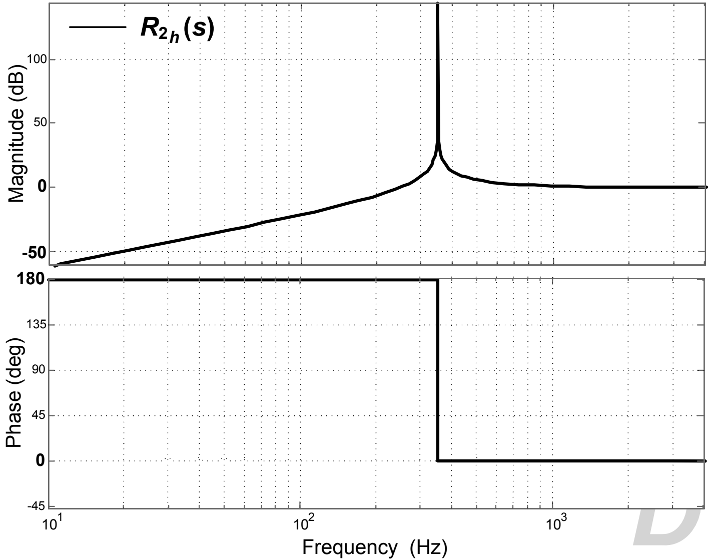

Pag. 49-50

Effects on Zeros of $R_{2_h}(s)$ (E methods)

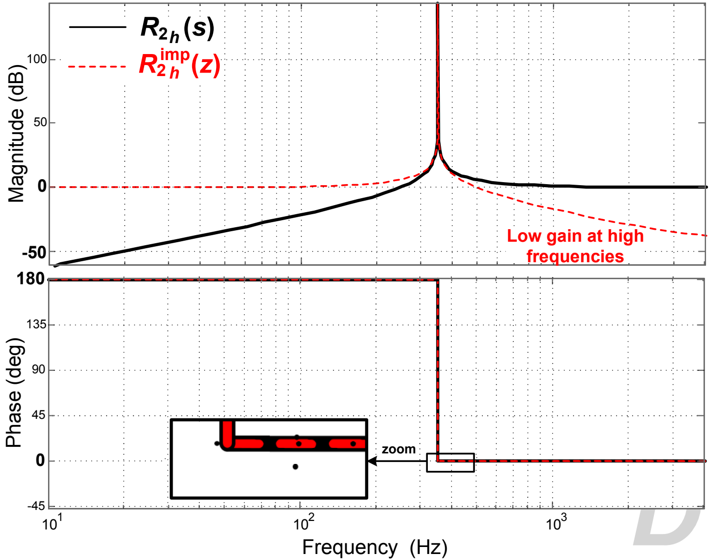

Pag. 49-50

Effects on Zeros of $R_{2_h}(s)$ (E methods)

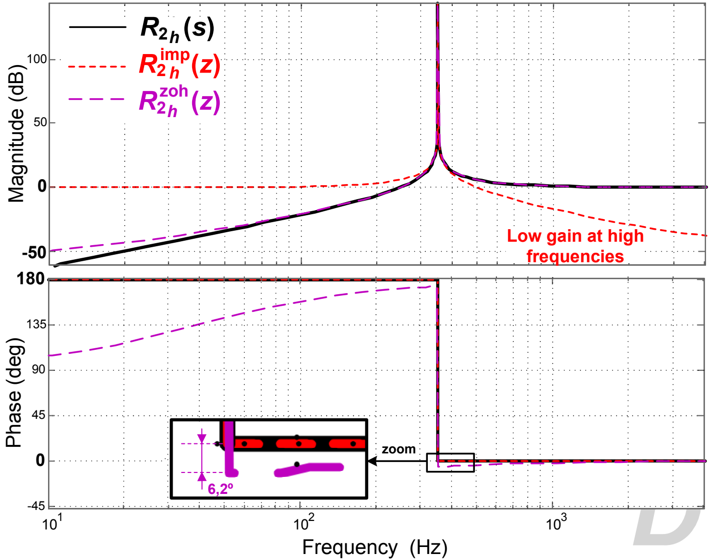

Pag. 49-50

Effects on Zeros of $R_{2_h}(s)$ (E methods)

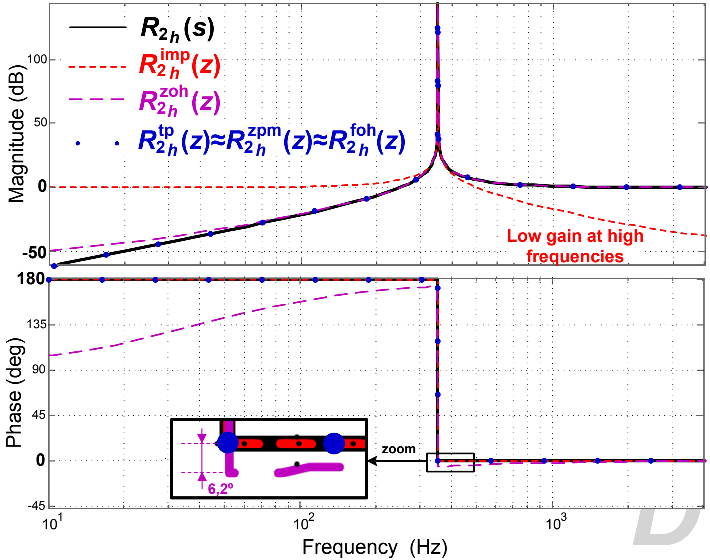

Pag. 49-50

Effects on Zeros of $G_{\mathrm{VPI}_h}(s)$ (D methods)

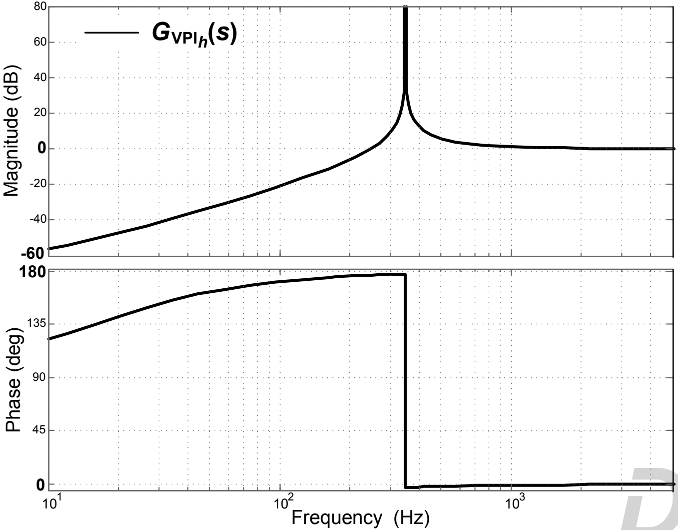

Pag.
50-51

Effects on Zeros of $G_{\mathrm{VPI}_h}(s)$ (D methods)

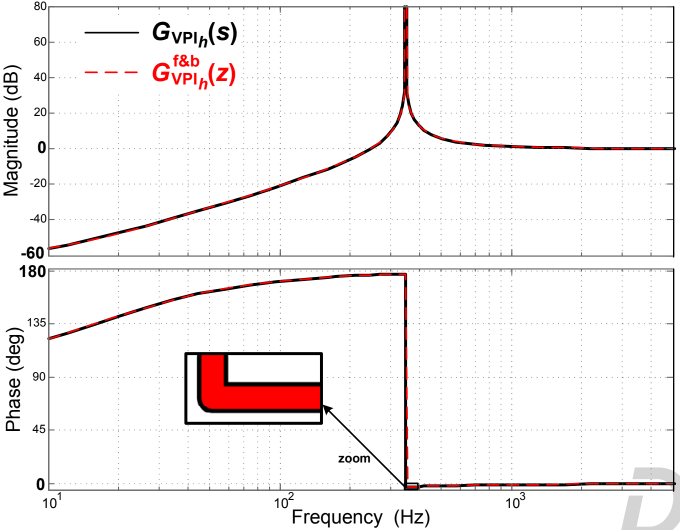

Pag.
50-51

Effects on Zeros of $G_{\mathrm{VPI}_h}(s)$ (D methods)

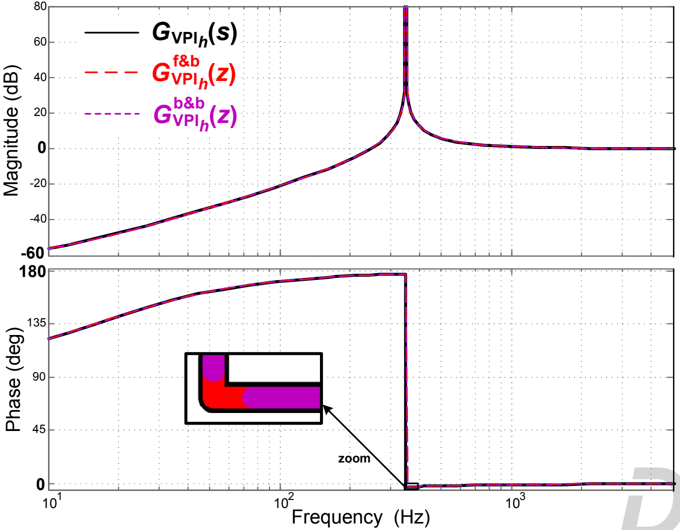

Pag. 50-51

Effects on Delay Compensation (E methods)

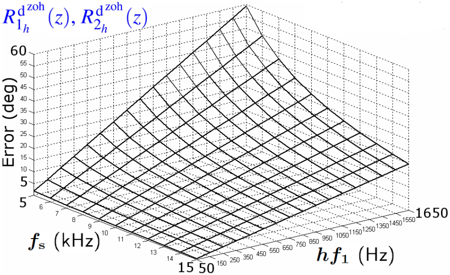

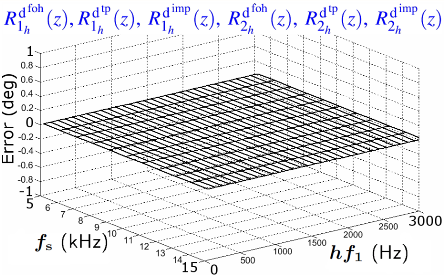

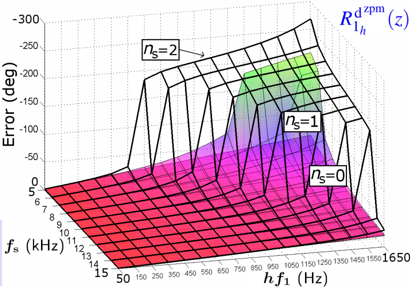

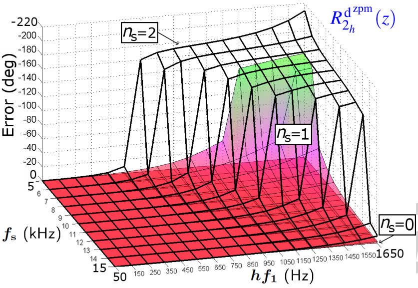

Pag. 54-57

Effects on Delay Compensation (D methods)

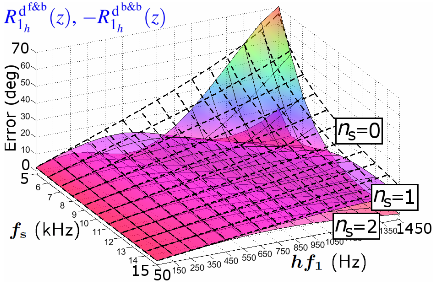

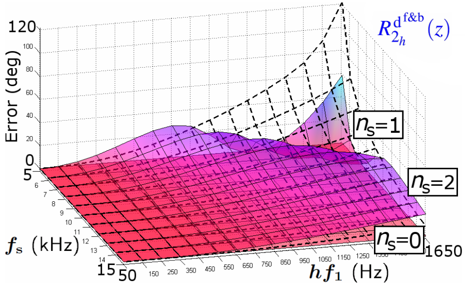

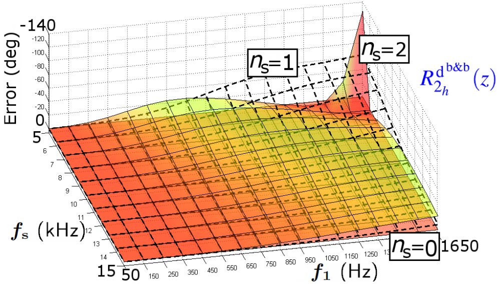

Pag. 57-58

Optimum Discrete-Time Implementations

No frequency adaptation		
No delay comp.	$G_{\mathrm{PR}_h}^{\mathrm{imp,foh,tp}}(z)$ $G_{\mathrm{VPI}_h}(z) = K_{\mathrm{P}_h}\, R_{2_h}^{\mathrm{foh,tp,zpm}}(z) + K_{\mathrm{I}_h}\, R_{1_h}^{\mathrm{imp,foh,tp}}(z)$	
Delay comp.	$G_{\mathrm{PR}_h}^{\mathrm{d\,imp,foh,tp}}(z)$ $G_{\mathrm{VPI}_h}^{\mathrm{d}}(z) = K_{\mathrm{P}_h}\, R_{2_h}^{\mathrm{d\,foh,tp}}(z) + K_{\mathrm{I}_h}\, R_{1_h}^{\mathrm{d\,imp,foh,tp}}(z)$	
Frequency adaptation		
No delay comp.	$G_{\mathrm{PR}_h}^{\mathrm{f\&b}}(z)$ $G_{\mathrm{VPI}_h}^{\mathrm{f\&b}}(z)$, $G_{\mathrm{VPI}_h}^{\mathrm{b\&b}}(z)$	*$G_{\mathrm{PR}_h}^{\mathrm{imp,foh,tp}}(z)$ *$G_{\mathrm{VPI}_h}(z) = K_{\mathrm{P}_h}\, R_{2_h}^{\mathrm{foh,tp,zpm}}(z) + K_{\mathrm{I}_h}\, R_{1_h}^{\mathrm{imp,foh,tp}}(z)$
Delay comp.	*$G_{\mathrm{PR}_h}^{\mathrm{d\,imp,foh,tp}}(z)$ *$G_{\mathrm{VPI}_h}(z) = K_{\mathrm{P}_h}\, R_{2_h}^{\mathrm{d\,foh,tp}}(z) + K_{\mathrm{I}_h}\, R_{1_h}^{\mathrm{d\,imp,foh,tp}}(z)$	

* Requires the on-line computation of $\cos(h\omega_1 T_s)$ terms as $h\omega_1$ varies.

Pag. 59-60

Experimental Setup (APF)

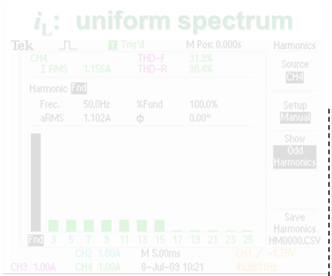

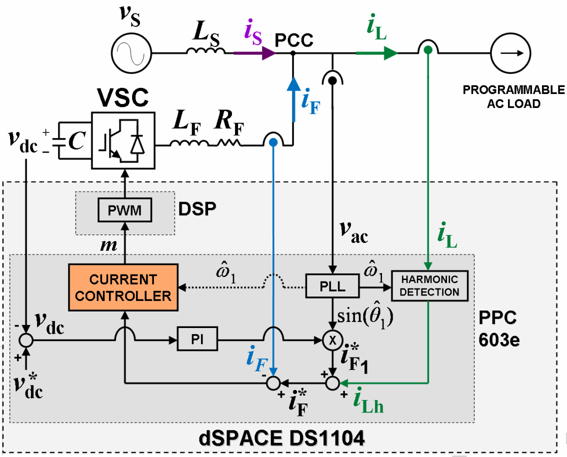

Pag.
60-62

Experimental Setup (APF)

i_L: uniform spectrum

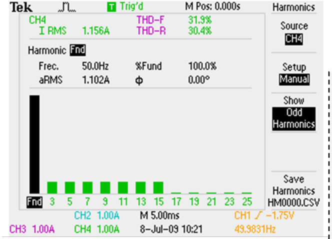

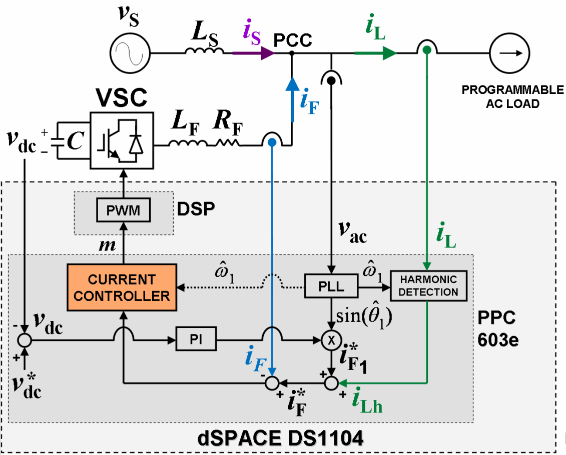

Pag. 60-62

Resonant Poles Displacement I

K_{P_T}

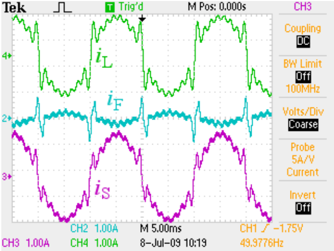

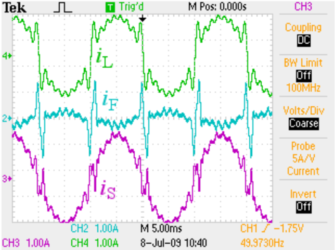

$G^{t}_{PR_h}(z)$

$G^{f\&b}_{PR_h}(z)$

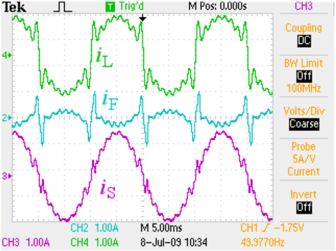

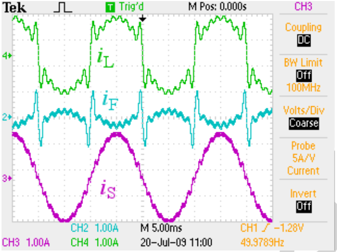

$G^{imp}_{PR_h}(z)$

Pag.
65-67

Resonant Poles Displacement II

K_{PT}

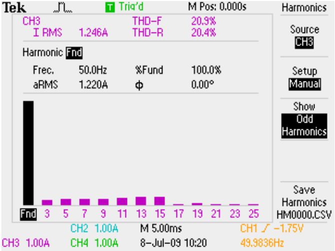

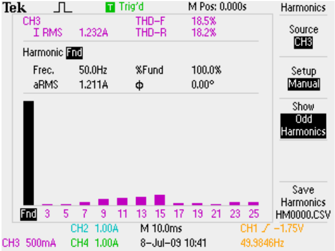

$G^{\mathrm{t}}_{\mathrm{PR}_h}(z)$

$G^{\mathrm{f\&b}}_{\mathrm{PR}_h}(z)$

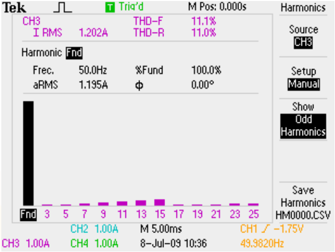

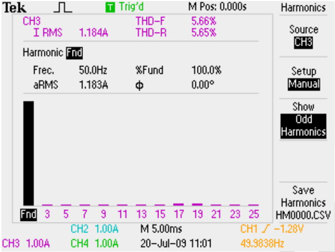

$G^{\mathrm{imp}}_{\mathrm{PR}_h}(z)$

Pag. 65-67

Discrete-Time Delay Compensation

$$G_{\mathrm{PR}_h}^{\mathrm{d\,imp}}(z)$$

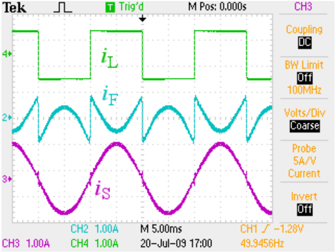

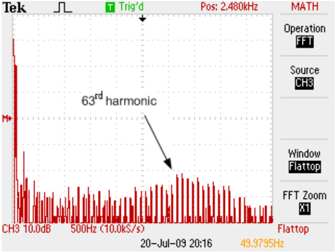

$$G_{\mathrm{VPI}_h}^{\mathrm{d\,imp-tp}}(z)$$

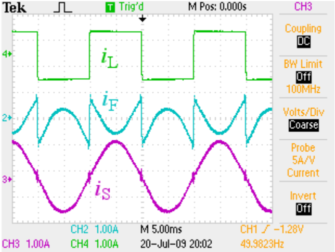

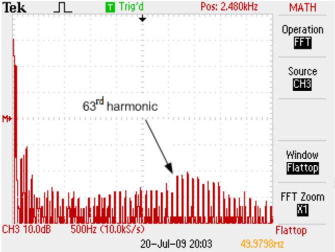

Pag.
67,69-70

Conclusions of Chapter II

- An exhaustive **study and comparison** of **discretization techniques** applied to resonant controllers has been presented, in terms of their effects on
  - **steady-state error**
  - **stability**
- It has been shown that the choice of discretization strategy is a **crucial** aspect for resonant controllers
- The **optimum** discrete-time implementations have been assessed

Pag. 72,74

Outline

Previous Schemes based on Two Integrators

$G_{\mathrm{PR}_h}(s)$

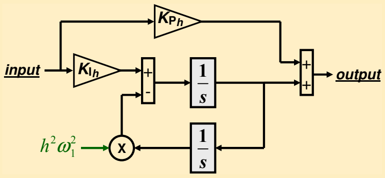

$G_{\mathrm{VPI}_h}(s)$

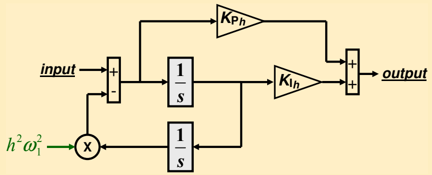

$G^{\mathrm{d}}_{\mathrm{PR}_h}(s)$

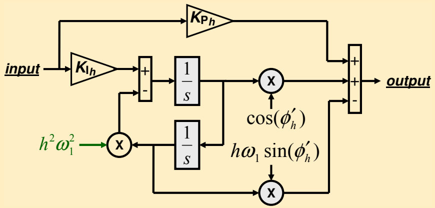

- Simple **frequency adaptation**
- Resonant poles deviation $\rightarrow$ **steady-state error**
- Leading angle ϕ_h deviation $\rightarrow$
  - anomalous **peaks**
  - **instability**

Pag. 75-77

Correction of Poles I

- **Accurate** resonant poles: $1-2z^{-1}\cos\left(h\omega_1 T_s\right)+z^{-2}$
- Schemes based on **2 int.**: $1-2z^{-1}\left(1-h^2\omega_1^2 T_s^2/2\right)+z^{-2}$

2nd order Taylor approx.

Proposed correction:

$$h^2\omega_1^2 \rightarrow C_h = 2\sum_{n=1}^{n_T/2}\frac{(-1)^{n+1}h^{2n}\omega_1^{2n}T_s^{2n-2}}{(2n)!} = \underbrace{\overbrace{h^2\omega_1^2 - h^4\frac{\omega_1^4 T_s^2}{12}}^{n_T=4} + h^6\frac{\omega_1^6 T_s^4}{360}}_{n_T=6} + \dots$$

$n_T = 4$: valid for most cases

Pag. 79-82

Correction of Poles I

- **Accurate** resonant poles: $1 - 2z^{-1}\boldsymbol{\cos(h\omega_1 T_s)} + z^{-2}$
- Schemes based on **2 int.**: $1 - 2z^{-1}\boldsymbol{(1 - \underline{h^2\omega_1^2}T_s^2/2)} + z^{-2}$

2nd order Taylor approx.

Proposed correction:

$$\underline{h^2\omega_1^2} \to C_h = 2\sum_{n=1}^{n_T/2} \frac{(-1)^{n+1} h^{2n}\omega_1^{2n}T_s^{2n-2}}{(2n)!} = \underbrace{\overbrace{h^2\omega_1^2 - h^4\frac{\omega_1^4 T_s^2}{12}}^{n_T = 4} + h^6\frac{\omega_1^6 T_s^4}{360}}_{n_T = 6} + \dots$$

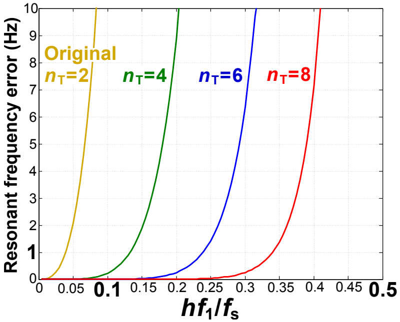

$n_T = 4$: valid for **most** cases

Pag. 79-82

Correction of Poles II

$G_{\mathrm{PR}_h}(z)$

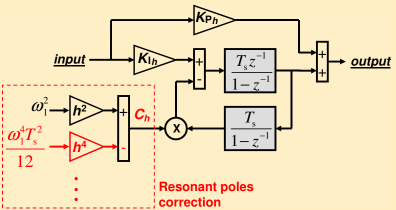

$G_{\mathrm{VPI}_h}(z)$

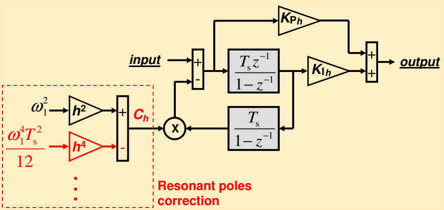

$G^{\mathrm{d}}_{\mathrm{PR}_h}(z)$

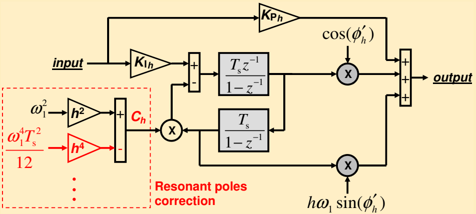

Pag. 79-82

Correction of Zeros

$$G^{\mathrm{d}}_{\mathrm{PR}_h}(s) = K_{\mathrm{P}_h} + K_{\mathrm{I}_h} \cdot \cdot \frac{s\,\cos(\phi'_h) - h\omega_1 \sin(\phi'_h)}{s^2 + h^2\omega_1^2}$$

- ϕ'_h: **target** leading angle
- ϕ_h: **actual** leading angle

Ideally:
$\phi_h = \phi'_h =$
$= -\angle G_{\mathrm{PL}}(e^{jh\omega_1 T_s})$

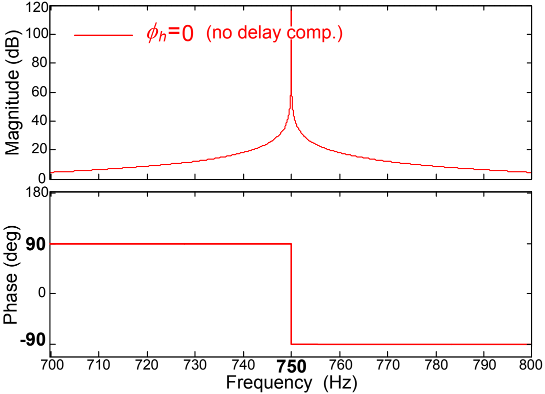

In previous **literature**:

1. **wrong target** (2 samples) $\rightarrow \phi'_h \neq -\angle G_{\mathrm{PL}}(e^{jh\omega_1 T_s})$
2. **discretization** $\rightarrow$ inaccuracy: $\phi_h \neq \phi'_h$

Pag.
78,82-83

Correction of Zeros

$$G^{\mathrm{d}}_{\mathrm{PR}_h}(s) = K_{\mathrm{P}_h} + K_{\mathrm{I}_h} \cdot \frac{s\ \cos(\phi'_h) - h\omega_1 \sin(\phi'_h)}{s^2 + h^2\omega_1^2}$$

- ϕ'_h: **target** leading angle
- ϕ_h: **actual** leading angle

Ideally:

$$\phi_h = \phi'_h = -\angle G_{\mathrm{PL}}(e^{jh\omega_1 T_s})$$

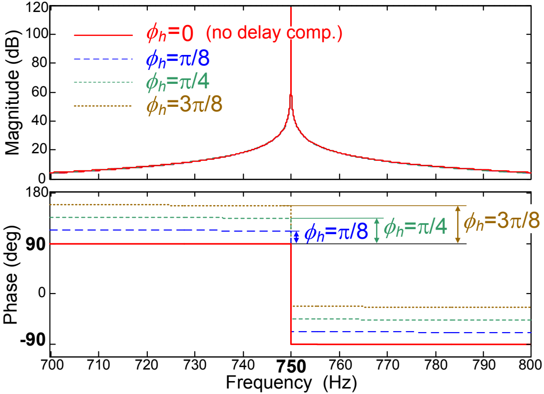

In previous **literature**:

1. **wrong target** (2 samples) $\rightarrow \phi'_h \neq -\angle G_{\mathrm{PL}}(e^{jh\omega_1 T_s})$
2. **discretization** $\rightarrow$ inaccuracy: $\phi_h \neq \phi'_h$

Pag. 78,82-83

Correction of Zeros

$$G^{\mathrm{d}}_{\mathrm{PR}_h}(s) = K_{\mathrm{P}_h} + K_{\mathrm{I}_h} \cdot \frac{s\ \cos(\phi'_h) - h\omega_1 \sin(\phi'_h)}{s^2 + h^2\omega_1^2}$$

- ϕ'_h: **target** leading angle
- ϕ_h: **actual** leading angle

Ideally:
$\phi_h = \phi'_h = -\angle G_{\mathrm{PL}}(e^{jh\omega_1 T_s})$

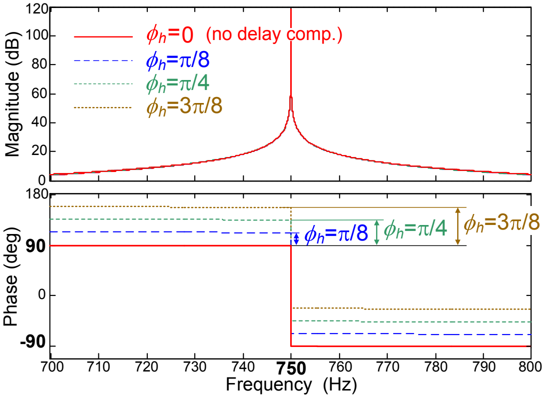

In previous **literature**:

1. **wrong target** (2 samples) $\rightarrow \phi'_h \neq -\angle G_{\mathrm{PL}}(e^{jh\omega_1 T_s})$
2. **discretization** $\rightarrow$ inaccuracy: $\phi_h \neq \phi'_h$

Pag.
78,82-83

Improvement in ϕ'_h Expression I

- **Objective:**

$$\phi'_h \approx \left|\angle G_{\mathrm{PL}}(e^{jh\omega_1 T_s})\right|$$

- 2 samples: **inaccurate**

- **Proposed:**

$$\phi'_h = \underbrace{\frac{\pi}{2}}_{\phi'_o} + \underbrace{\frac{3}{2}T_s}_{\lambda}$$

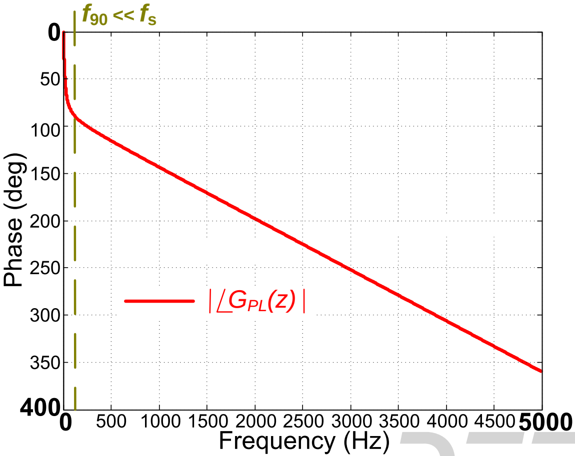

Pag. 83-85

Improvement in ϕ'_h Expression I

- **Objective:**

$$\phi'_h \approx \left|\angle G_{\mathrm{PL}}\left(e^{jh\omega_1 T_s}\right)\right|$$

- 2 samples: **inaccurate**

- **Proposed:**

$$\phi'_h = \underbrace{\frac{\pi}{2}}_{\phi'_o} + \underbrace{\frac{3}{2}T_s}_{\lambda}$$

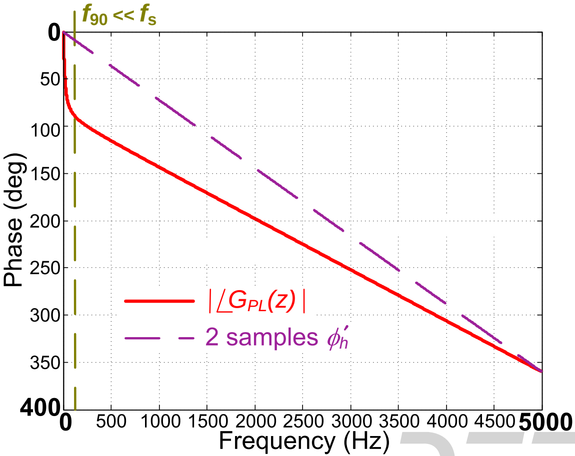

Pag.
83-85

Improvement in ϕ'_h Expression I

- **Objective:**

$$\phi'_h \approx \left|\angle G_{\mathrm{PL}}(e^{jh\omega_1 T_s})\right|$$

- 2 samples: **inaccurate**

- **Proposed:**

$$\phi'_h = \underbrace{\frac{\pi}{2}}_{\phi'_o} + \underbrace{\frac{3}{2}}_{\lambda} T_s$$

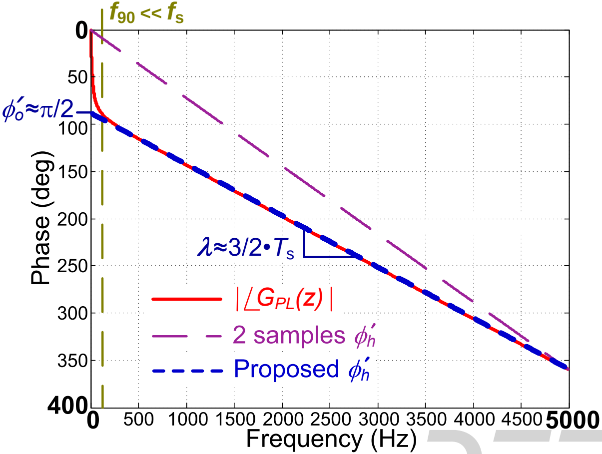

Pag. 83-85

Improvement in ϕ_h' Expression II

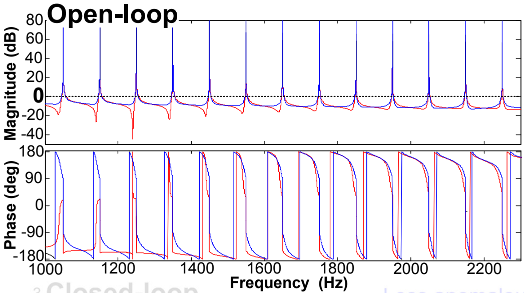

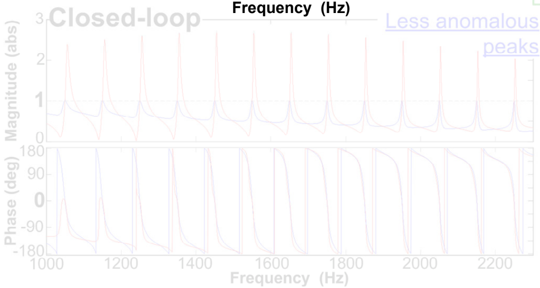

Greater phase margin

Proposed ϕ_h'

2 samples ϕ_h'

Pag. 85-87

Improvement in ϕ_h' Expression II

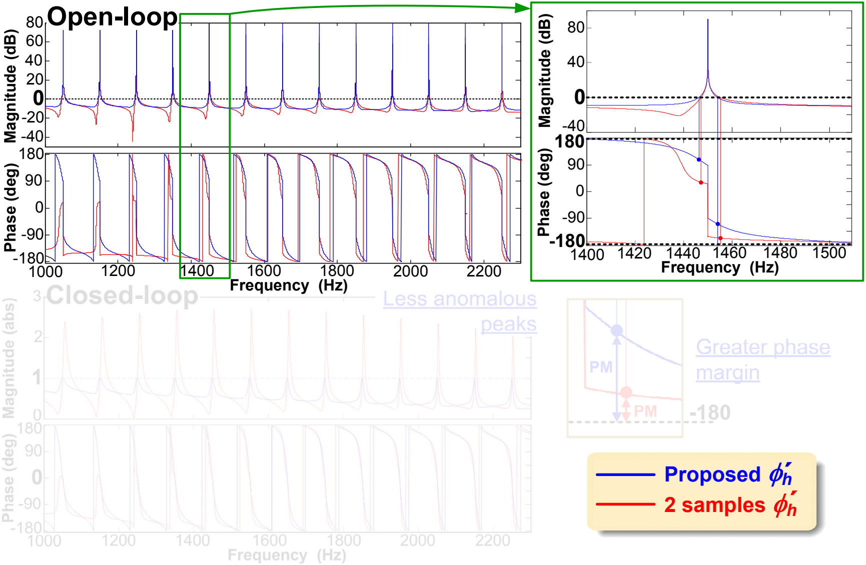

Pag. 85-87

Improvement in ϕ_h' Expression II

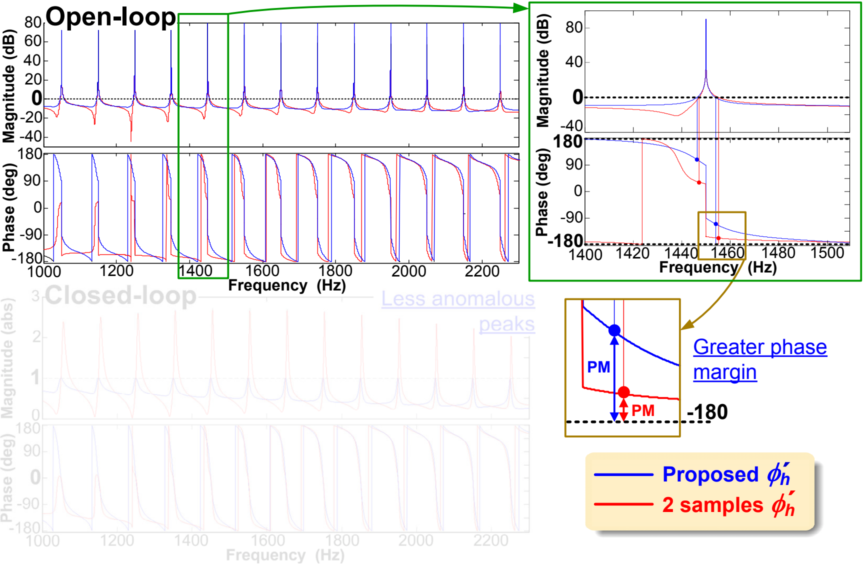

Pag. 85-87

Improvement in ϕ'_h Expression II

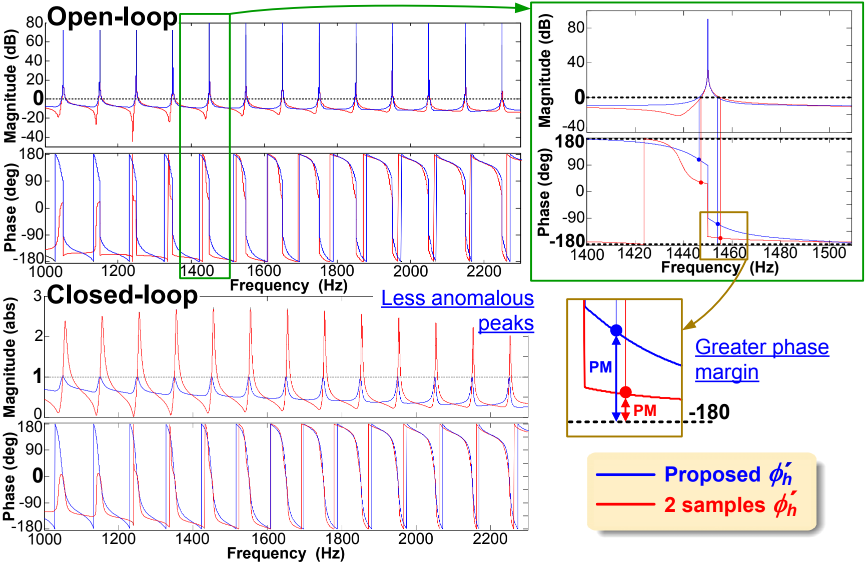

Pag. 85-87

Correction of ϕ_h Error Due to Discretization I

1^{st} order **Taylor** approximation centered at **0**

$$z^{-1}\left[\,\mathbf{\cos(\phi'_h) - h\omega_1 T_s \sin(\phi'_h)}\,\right] - z^{-2}\cos(\phi'_h) \longleftarrow z^{-1}\,\mathbf{\cos(h\omega_1 T_s + \phi'_h)} - z^{-2}\cos(\phi'_h)$$

Original delay compensation

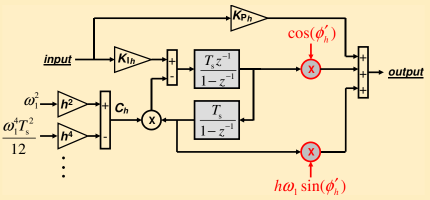

Accurate

Optimized

1^{st} order **Taylor** approximation centered at $h\omega_{1n}$

- a_h-d_h: pre-calculated constants

Pag. 87-90

Correction of ϕ_h Error Due to Discretization I

1^{st} order **Taylor** approximation centered at **0**

$$z^{-1}\left[\,\boldsymbol{\cos(\phi'_h) - h\omega_1 T_s \sin(\phi'_h)}\,\right] - z^{-2}\cos(\phi'_h) \longleftarrow z^{-1}\boldsymbol{\cos(h\omega_1 T_s + \phi'_h)} - z^{-2}\cos(\phi'_h)$$

Original delay compensation

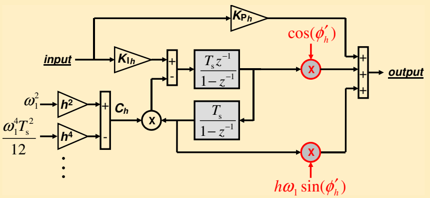

Accurate

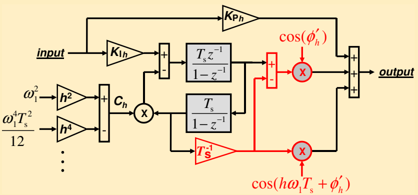

Optimized

1^{st} order **Taylor** approximation centered at $h\omega_{1n}$

- a_h-d_h: pre-calculated constants

Pag. 87-90

Correction of ϕ_h Error Due to Discretization I

1^{st} order **Taylor** approximation centered at **0**

$$z^{-1}\left[\boldsymbol{\cos(\phi'_h) - h\omega_1 T_s \sin(\phi'_h)}\right] - z^{-2}\cos(\phi'_h) \longleftarrow z^{-1}\boldsymbol{\cos(h\omega_1 T_s + \phi'_h)} - z^{-2}\cos(\phi'_h)$$

Original delay compensation

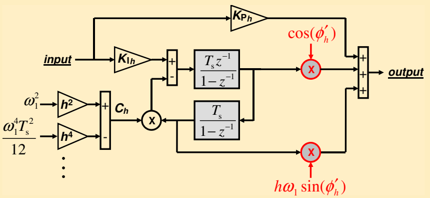

Accurate

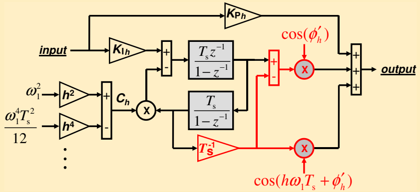

Optimized

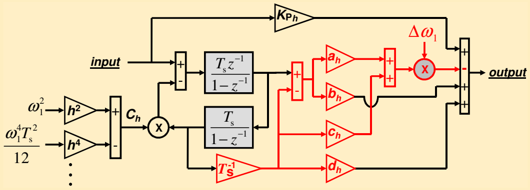

1^{st} order **Taylor** approximation centered at $h\omega_{1n}$

- a_h-d_h: pre-calculated **constants**

Pag. 87-90

Correction of ϕ_h Error Due to Discretization II

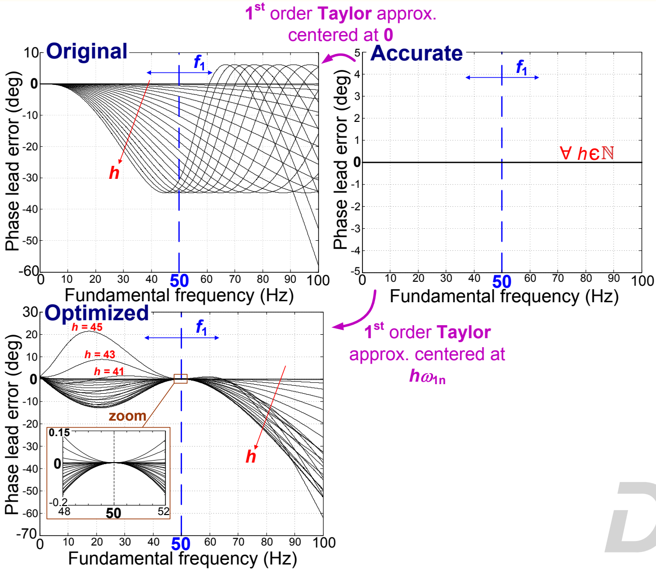

Pag. 90-92

Correction of Poles I

$n_{\mathrm{T}}=2$
(no correction)
25.8 µs

$n_{\mathrm{T}}=4$
29.8 µs

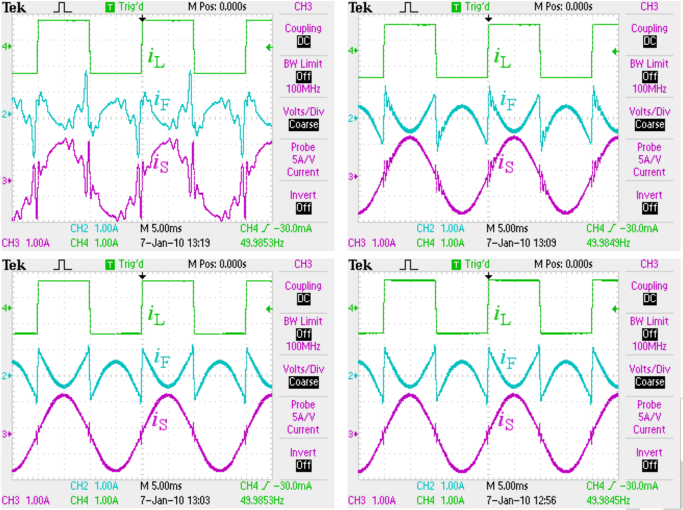

$n_{\mathrm{T}}=6$
32.1 µs

$n_{\mathrm{T}}=8$
34.7 µs

Pag.
92-96

Correction of Poles II

$n_T = 2$
(no correction)
25.8 µs

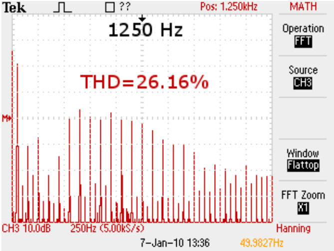

$n_T = 4$
29.8 µs

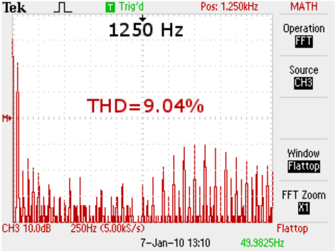

$n_T = 6$
32.1 µs

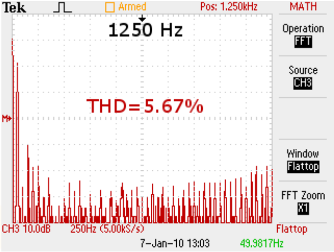

$n_T = 8$
34.7 µs

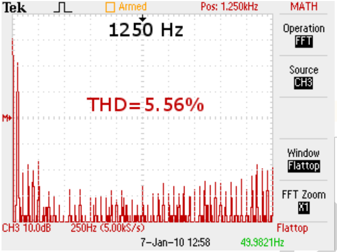

Pag. 92-96

Correction of Zeros

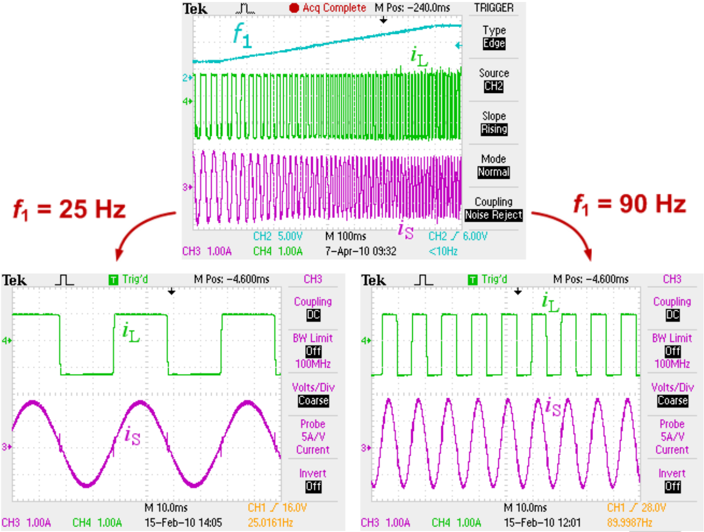

Pag.
97-98

Conclusions of Chapter III

- Enhanced digital implementations of resonant controllers based on two integrators are contributed, with an **optimized** trade-off between **accuracy** and **simplicity**.
  - Correction of poles: improvement in **steady-state error**
  - Correction of zeros: improvement in **stability margins**
  - The advantages of the originals are maintained: **low computational burden** and **easy frequency adaptation**
- The steady-state error as a function of the order of Taylor series approximation of the poles has been studied. A **fourth order** is satisfactory for most cases
- An **expression** is proposed for the **target leading angle**, in order to achieve a better compensation of the plant phase lag

Pag.
98-99

Outline

Limitations of Previous Approaches

PR controllers

- PM_{P} is usually employed as indicator of **stability**. However, when there are **more 0 dB crossings** (e.g., high-power, selective control...), PM_{P} is no longer valid
- Usually, **phase margins** are **optimized**. However:
  - the phase margin is a **less reliable** indicator than the sensitivity peak $1/\eta$
  - closed-loop **anomalous peaks** are directly related to η, not to phase margin

VPI controllers

- **No** methods have been proposed to measure and optimize **proximity to instability** and closed-loop **anomalous peaks**
- Ambiguity in ϕ'_h selection: leading angles of **1 & 2 samples** have been proposed

Nyquist Diagrams of PR Controllers I

· · · $K_{P_T} G_{PL}(z)$ (only proportional gain)

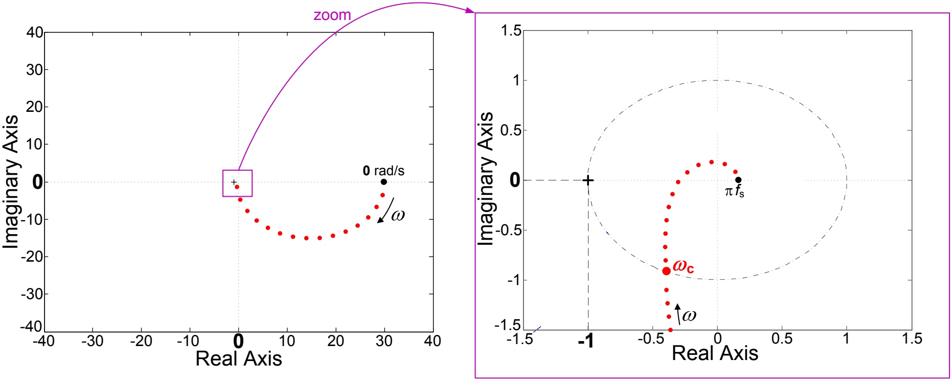

- K_{P_T} defines ω_c, PM_P, GM_P and η_P
- $PM_h \leq PM_P$, $GM_h \leq GM_P$ and $\eta_h \leq \eta_P$

Pag.
104-107

Nyquist Diagrams of PR Controllers I

· · · $K_{P_T} G_{PL}(z)$ (only proportional gain)

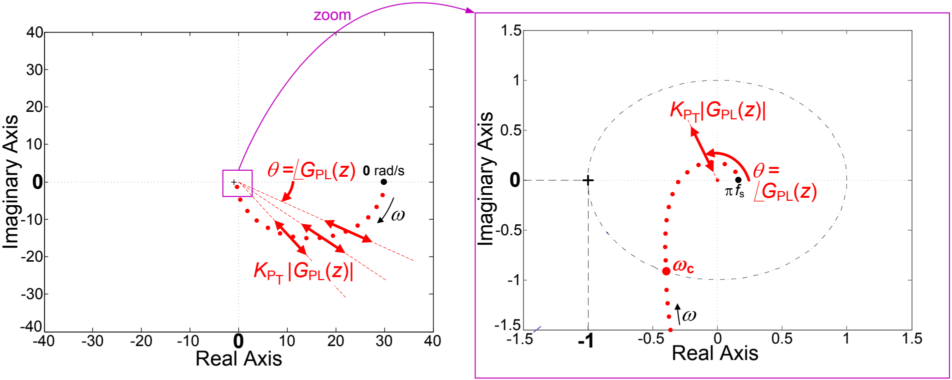

- K_{P_T} defines ω_c, PM_P, GM_P and η_P
- $PM_h \le PM_P$, $GM_h \le GM_P$ and $\eta_h \le \eta_P$

Pag.
104-107

Nyquist Diagrams of PR Controllers I

$\cdots\ K_{P_T} G_{PL}(z)$ (only proportional gain)

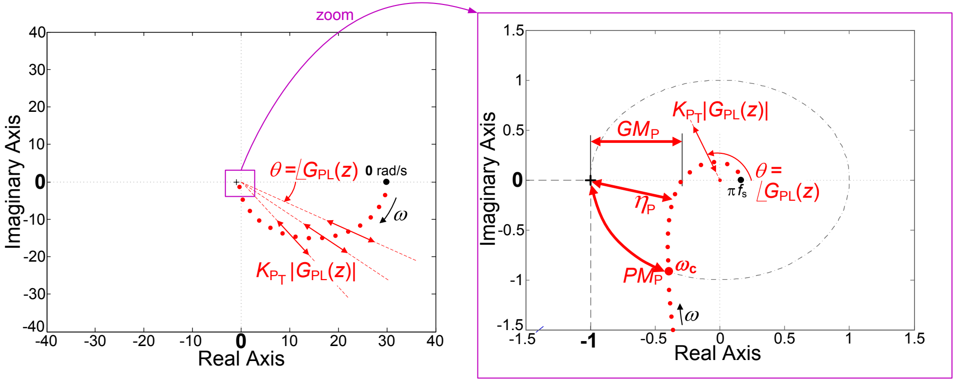

- K_{P_T} defines ω_c, PM_P, GM_P and η_P
- $PM_h \leq PM_P$, $GM_h \leq GM_P$ and $\eta_h \leq \eta_P$

Pag.
104-107

Nyquist Diagrams of PR Controllers I

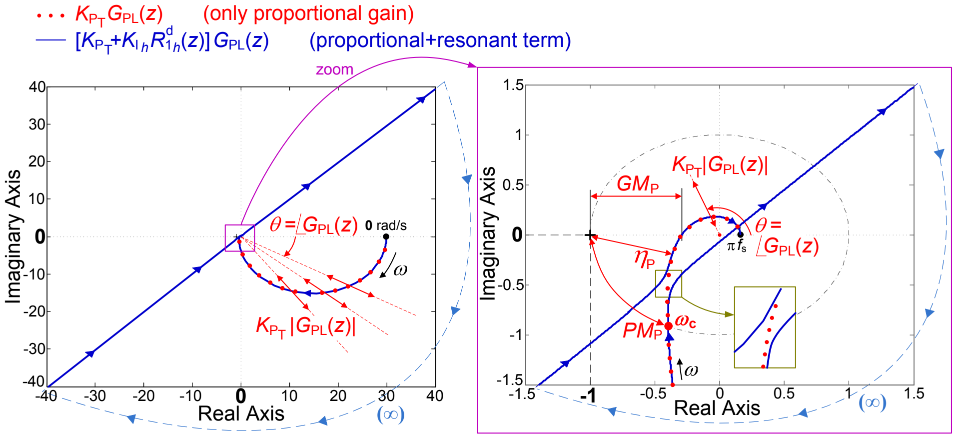

- K_{P_T} defines ω_c, PM_P, GM_P and η_P
- $PM_h \leq PM_P$, $GM_h \leq GM_P$ and $\eta_h \leq \eta_P$

Pag. 104-107

Nyquist Diagrams of PR Controllers I

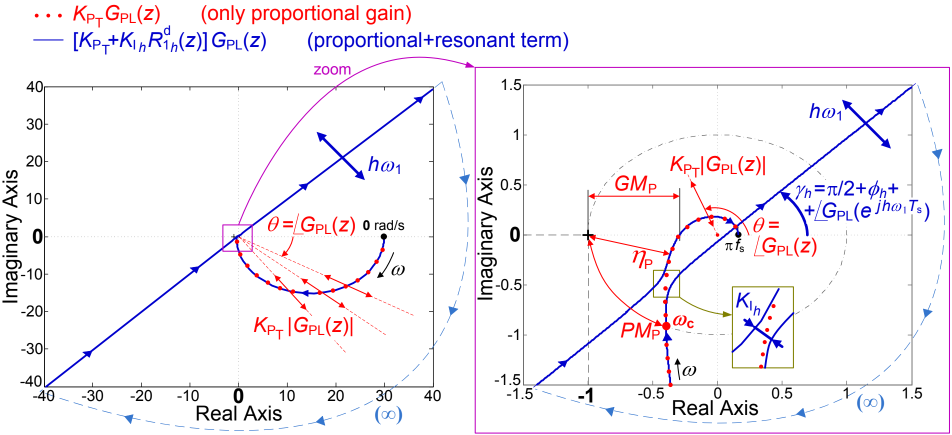

- K_{P_T} defines ω_c, PM_P, GM_P and η_P
- $PM_h \leq PM_P$, $GM_h \leq GM_P$ and $\eta_h \leq \eta_P$

Pag. 104-107

Nyquist Diagrams of PR Controllers I

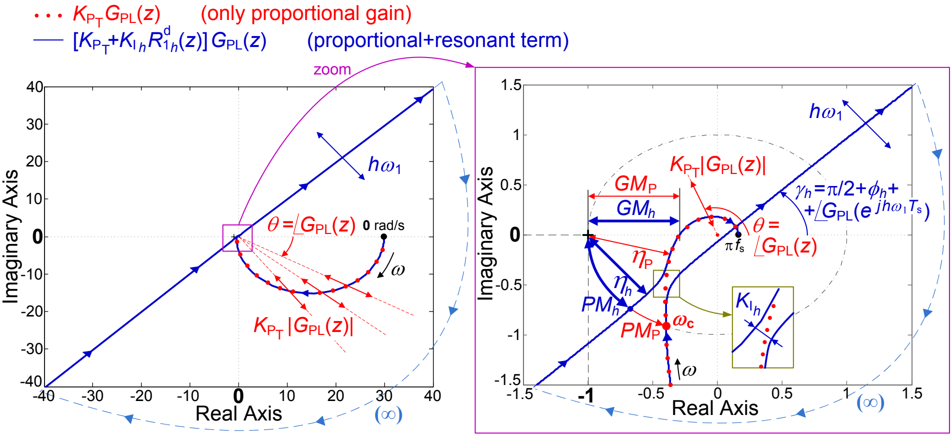

- K_{P_T} defines ω_c, PM_P, GM_P and η_P
- $PM_h \le PM_P$, $GM_h \le GM_P$ and $\eta_h \le \eta_P$

Pag. 104-107

Nyquist Diagrams of PR Controllers II

- $GM_h > 0$ and $PM_{\mathrm{P}} > 0$, but system is **unstable**
- $GM_h < 0$, but system is **stable**
- $\phi'_h = 0$ and $h\omega_1 > \omega_{\mathrm{c}}$, but system is **stable**

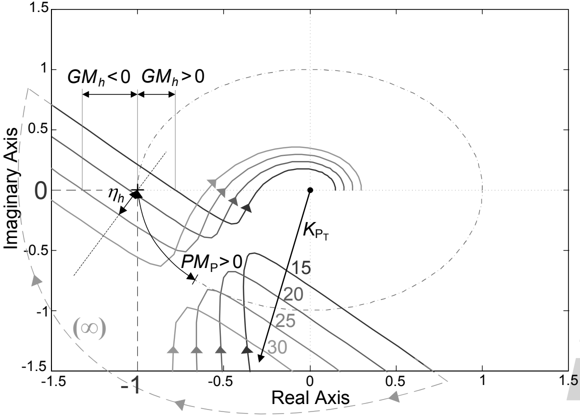

Pag.
106-107

Nyquist Diagrams of PR Controllers II

- $GM_h > 0$ and $PM_P > 0$, but system is **unstable**
- $GM_h < 0$, but system is **stable**
- $\phi'_h = 0$ and $h\omega_1 > \omega_c$, but system is **stable**

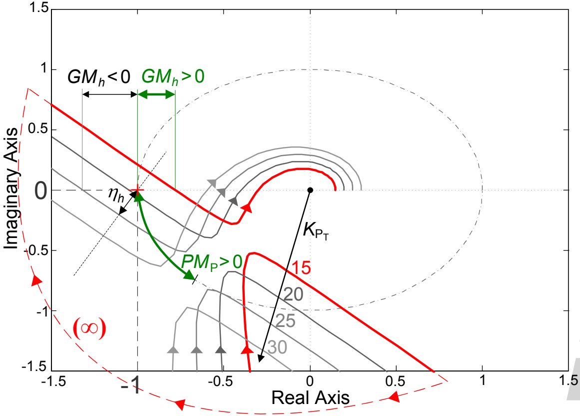

Pag.
106-107

Nyquist Diagrams of PR Controllers II

- $GM_h > 0$ and $PM_P > 0$, but system is **unstable**
- $GM_h < 0$, but system is **stable**
- $\phi'_h = 0$ and $h\omega_1 > \omega_c$, but system is **stable**

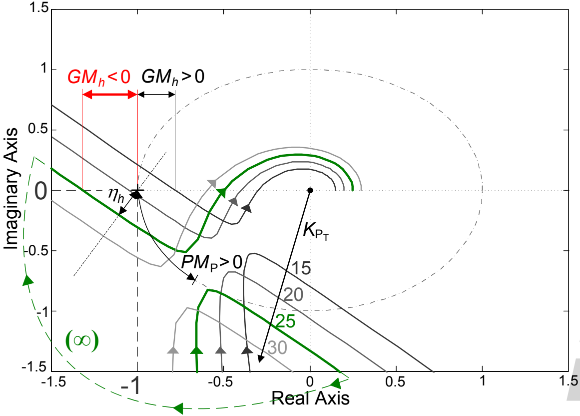

Pag. 106-107

Nyquist Diagrams of PR Controllers II

- $GM_h > 0$ and $PM_\mathrm{P} > 0$, but system is **unstable**
- $GM_h < 0$, but system is **stable**
- $\phi'_h = 0$ and $h\omega_1 > \omega_c$, but system is **stable**

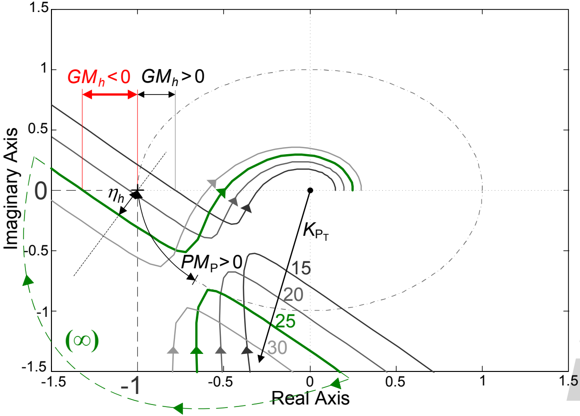

Nyquist Diagrams of PR Controllers III

η_h provides more information about the actual **proximity to instability** than PM_h

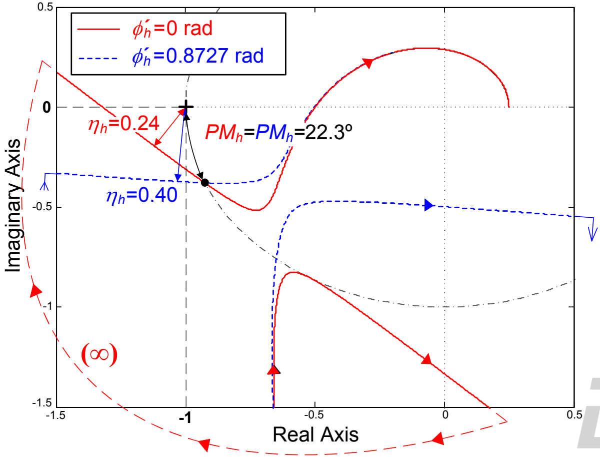

Pag. 106,108

Nyquist Diagrams of PR Controllers IV

- $\phi'_h = -\angle G_{\mathrm{PL}}(e^{jh\omega_1 T_s})$ is usually pursued, but it is **not** the optimum
- **Objective:** ϕ'_h such that η_h becomes **maximum**, i.e., $\eta_h = \eta_{\mathrm{P}}\ \forall h$

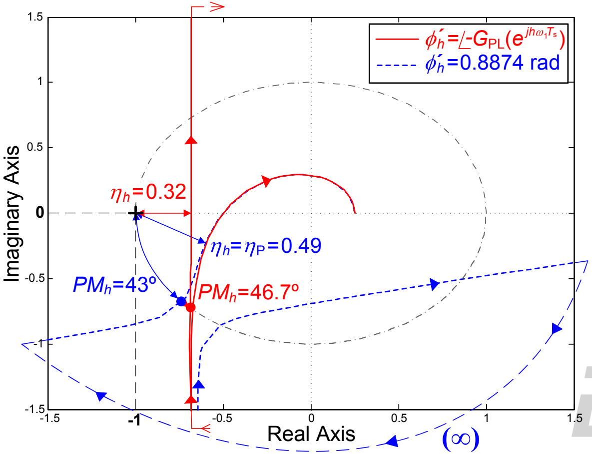

Pag. 106-108

Nyquist Diagrams of PR Controllers V

η **defines:**

- Proximity to **instability**
- **Oscillations** during transients (damping)
- Maximum steady-state **error**

$$\mathbf{max}\{|S(z)|\} = \mathbf{1}/\boldsymbol{\eta} \Leftarrow \begin{cases} |D(z)| \leq \eta \\ S(z) = E(z)/I^*(z) = 1/D(z) \end{cases}$$

$\boldsymbol{\eta}_{\mathbf{P}}$ is set by $\boldsymbol{K}_{\mathbf{P_T}}$:

$$\boldsymbol{K}_{\mathbf{P_T}} = F_1\left(\boldsymbol{\eta}_{\mathbf{P}}, T_{\mathrm{s}}, R_{\mathrm{F}}, L_{\mathrm{F}}\right)$$

Pag.
106-108

Nyquist Diagrams of VPI Controllers

- $|G_{\mathrm{PL}}(z)|$ is cancelled
- $\phi_h = \phi'_h + \arctan(h\omega_1 L_{\mathrm{F}}/R_{\mathrm{F}})$

} **Greater stability** margins and **easier design** than PR

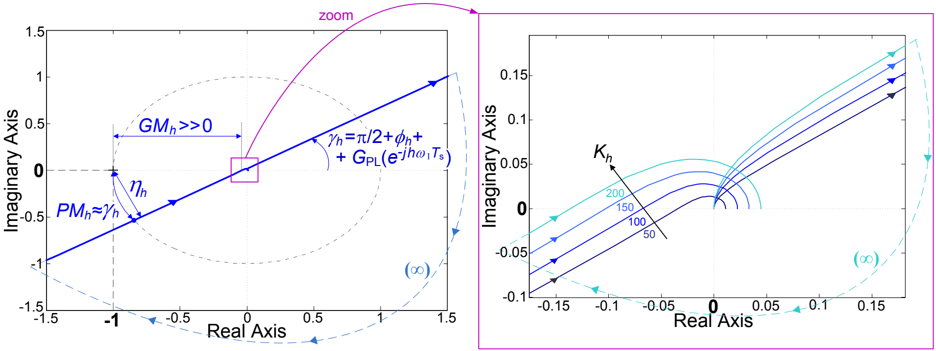

Stable $\Leftrightarrow$ $\gamma_h > 0 \quad \forall h$

Pag. 110-112

Relation in PR Controllers

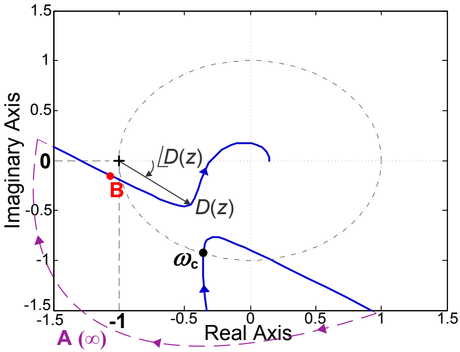

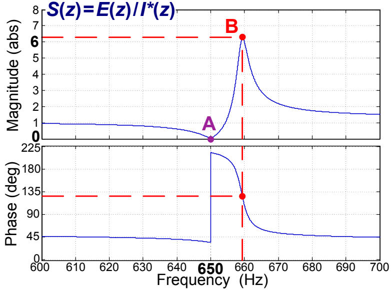

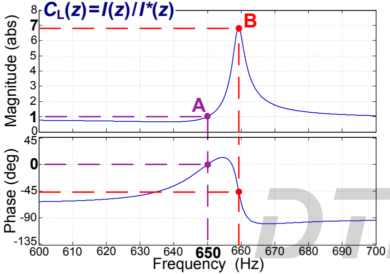

- A: $h\omega_1$
- B: $D(e^{j\omega_B T_s}) = \eta_h$

Pag.
113,115-117

Relation in PR Controllers

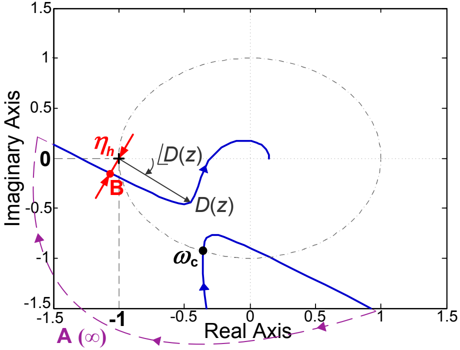

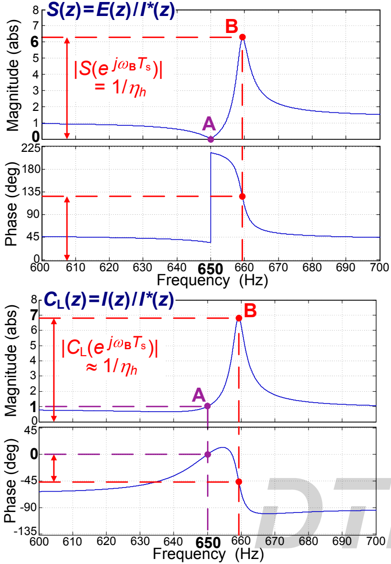

- A: $h\omega_1$
- B: $D(e^{j\omega_B T_s}) = \eta_h$

Pag. 113,115-117

Relation in VPI Controllers

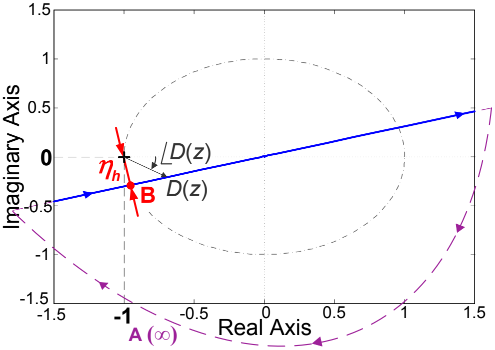

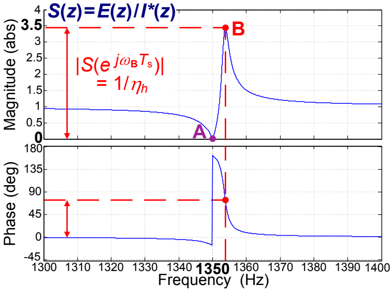

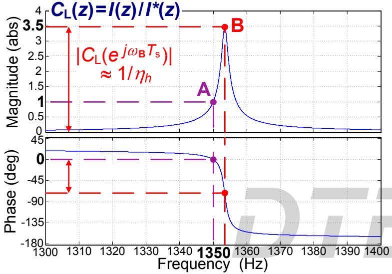

- A: $h\omega_1$
- B: $D(e^{j\omega_B T_s}) = \eta_h$

Pag.
113,115-117

Minimization of $S(z)$ in PR Controllers

- **Objective:** ϕ'_h such that η_h becomes **maximum**, i.e., $\eta_h = \eta_{\mathrm{P}}\ \forall h$
- **Solution:** $\phi'_h = -\angle G_{\mathrm{PL}}(e^{jh\omega_1 T_s}) + \angle D(e^{jh\omega_1 T_s})$

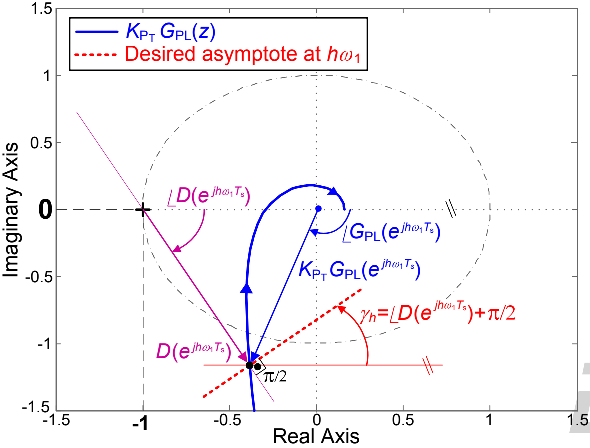

Pag. 117-118

Minimization of $S(z)$ in VPI Controllers

Optimum: $\phi'_h = \frac{3}{2}T_s \Leftarrow \begin{cases} \text{max. } \eta_h \Rightarrow \gamma_h = \frac{\pi}{2} \Rightarrow \phi_h = -\angle G_{PL}(e^{jh\omega_1 T_s}) \\ \phi_h = \phi'_h + \arctan(h\omega_1 L_F / R_F) \end{cases}$

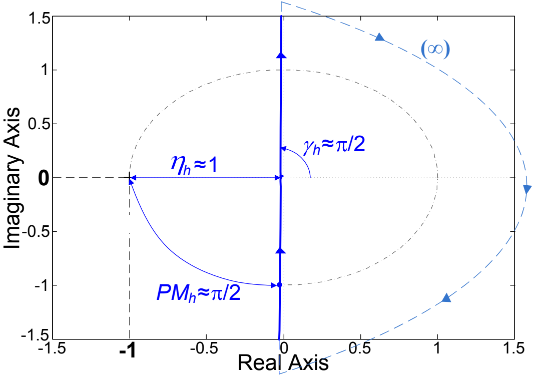

Pag. 118-119

Test I

Objective of Test I: prove the **sensitivity minimization** around $h\omega_1$ achieved by the **proposed** ϕ'_h expressions

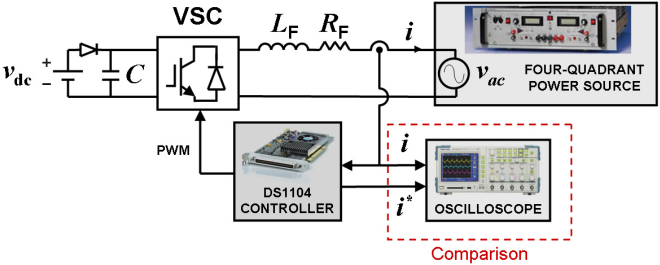

Pag. 119-120

Test I (PR Controller)

650 Hz | 656 Hz

$\phi'_h = 0$

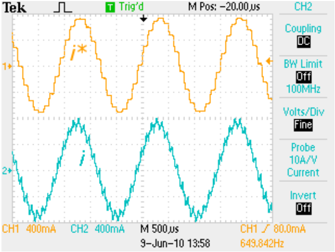

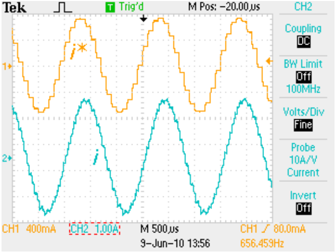

Proposed ϕ'_h

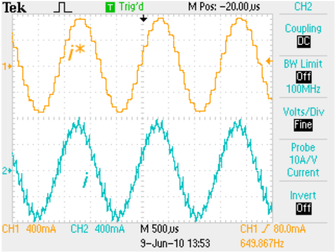

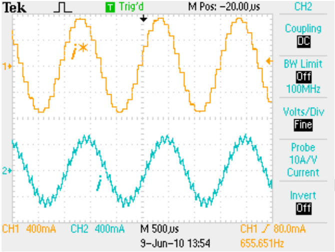

Pag. 120-123

Test I (VPI Controller)

1300 Hz | 1303 Hz

$\phi'_h = 0$

Proposed ϕ'_h

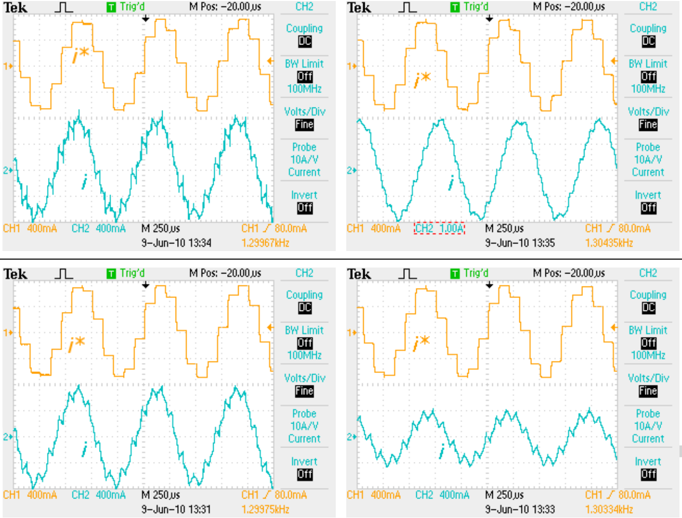

Pag. 123-124

Test II (Transient)

PR

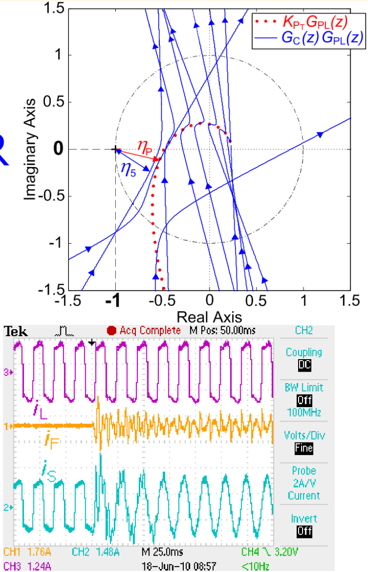

VPI

Pag.
125-129

Test II (Transient)

PR

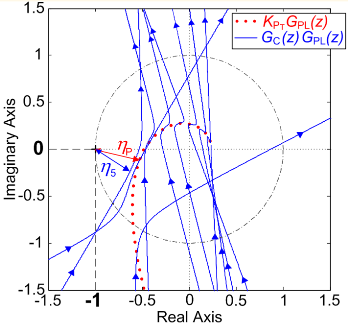

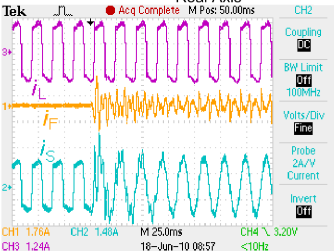

VPI

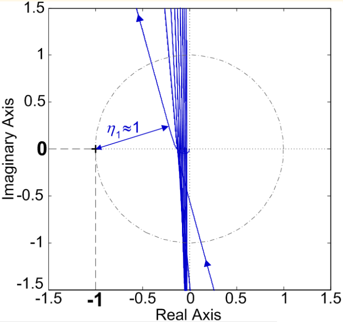

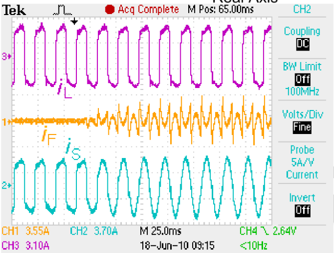

Pag.
125-129

Test II (Steady-State)

THD=28.4 %

PR

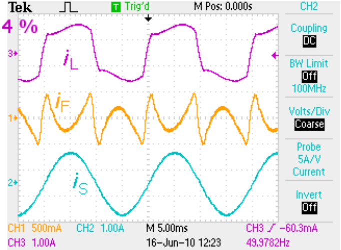

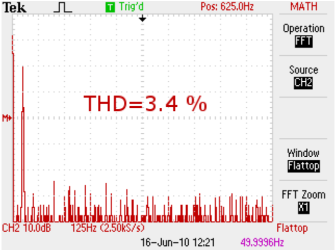

VPI

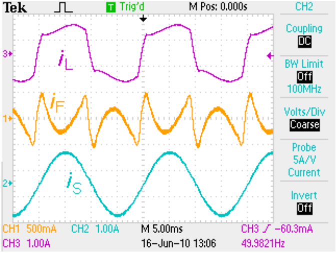

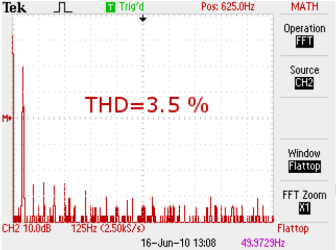

Pag.
123-127

Conclusions of Chapter IV

- **PR** and **VPI** controllers, including delay compensation, are analyzed my means of **Nyquist diagrams**. The effect of each freedom degree on the trajectories is studied, and their relation with the **sensitivity function** and its peak value is assessed
- Optimization of the **sensitivity peak** permits to achieve a better performance and stability in resonant controllers than optimization of the **gain** or **phase margins**
- A **systematic method**, supported by closed-form analytical expressions, is proposed to optimize
  - **stability**
  - avoidance of closed-loop **anomalous peaks**
  - **transient response** (greater damping of frequencies at which the trajectory is closer to the critical point)

Pag.
128

Outline

Conclusions

- An exhaustive **study and comparison** of **discretization techniques** applied to resonant controllers has been presented, in terms of
  - steady-state error
  - stability
- **Implementations** based on **two integrators**, that overcome the issues of the original ones, have been proposed. They achieve an optimized tradeoff between
  - accuracy
  - simplicity
- It is proved that to minimize the **sensitivity peak** permits a better performance and stability in resonant controllers than to maximize the gain or phase margins. A **systematic method** is proposed to obtain
  - high **stability**
  - reduced closed-loop **anomalous peaks**
  - reduced oscillations in **transients**

Future Research

- Optimization of **transient** response for **distributed** power generation systems
- **Torque ripple** minimization
- Injection of current harmonics in **multi-phase** drives for **fault-tolerance** operation and **increase of average torque**
- Active compensation of undesired current components caused by **dead-time** in **multi-phase** converters

Digital Resonant Current Controllers for Voltage Source Converters

Author: Alejandro Gómez Yepes
Director: Jesús Doval Gandoy

Department of Electronics Technology, University of Vigo,

14 December 2011

Dissertation submitted for the degree of
Doctor of Philosophy at the University of Vigo

"Doctor Europeus" mention

Pag.
132